The effect of dolutegravir on adipose tissue and adipose tissue health

by

Johanna Adriana Coetzee

Thesis presented in fulfilment of the requirements for the degree of Master of Science in the Faculty of Medicine and Health Science at Stellenbosch University.

Supervisor: Prof. Carine Smith

Co-supervisor: Dr Kelly Shirley Petersen-Ross

December 2022

<u>Declaration</u>

By submitting this thesis electronically, I declare that the entirety of the work contained therein is my own, original work, that I am the sole author thereof (save to the extent explicitly otherwise stated), that reproduction and publication thereof by Stellenbosch University will not infringe any third party rights and that I have not previously in its entirety or in part submitted it for obtaining any qualification. Date: ......26.08.2022....

Abstract

Introduction: Dolutegravir, an integrase strand transfer inhibitor (INSTI), forms part of the first-line antiretroviral (ARV) therapy. Despite low cost, fewer drug-drug interactions and minimal reported side effects, dolutegravir use has clinically been associated with weight gain. The significance of this in terms of   adipose- and overall patient health remains to be fully elucidated.

Methods: The effects of dolutegravir on the adipose tissue health were assessed in a 12-week treatment intervention study in Wistar rats, allowing an assessment of risk profile for dolutegravir in the absence of potential confounding effects of retroviral infection or other ARV agents commonly found in combination therapy. Dolutegravir was administered as a human equivalent dose set in jelly blocks, once daily for 12 weeks, starting at 8 weeks of age. Visceral adipose tissue morphology and fibrosis profile, adipokine and inflammatory cytokine levels were assessed.

Results: Dolutegravir did not change the rate of body mass increase in the rats (when compared to a placebo group). Females presented to have smaller adipocyte size and increased adiponectin secretion – more pronounced in the treated group compared to the controls. While pro-inflammatory cytokines (TNF-α and MCP-1) were also elevated in both the female groups compared to the males.

Conclusion: Current data illustrates that in terms of potential effects of dolutegravir on AT health, females seem more vulnerable to undesired longer term outcome. The overall small effect sizes seen is in line with a chronic, low-grade dysregulation which may predispose dolutegravir-treated patients to development of co-morbidities with a chronic inflammatory character.

Opsomming

Inleiding: Dolutegravir (DTG), is onlangs ingesluit as deel van die voorlyn antiretroviralemiddels op die mark. Ten spyte van laer kostes, verlaagde risiko van interaksie met ander medikasie en 'n afname in geraporteerde neweeffekte, word die gebruik van DTG steed geassosieer met merkbare gewigstoename. Gewigstoename gaan gepaard met lae graadse lokale en sistemiese inflammasie - Van daar die belangom die effek van die DTG en DTG verwante gewigstoename in vetweefsel, en die gesondheid van individue te evalueer.

Metodes: Die effek van DTG op vetweefsel is geavalueer deur middel van 'n 12-week rotstudie.Die studie het bestaan uit 24 Rotte – wat uit 12 vroulik en 12 manlike diere bestaan het. Die rotte is verder opgedeel in 'n groep wat DTG belandeling ontvang het en 'n kontrole groep (Die kontrole groep het fopmedikasie (placebo) ontvang). Die DTG is in 'n jellieblokkie gestol en daagliks vir die rotte gevoer. Die dosis was ekwiwalent aan die eens-daaglikse dosis wat pasiënte met MIV ontvang. Die studie is gedoen in die afwesigheid van MIV en kombinasie antiretroviralemiddels om die effekte wat deur DTG veroosaak word optimaal en noukeurig vas te stel. Viserale vet is gebruik om die morfologie en fibrose indeks te ondersoek. Verder is die vlakke van verskillende pro-inflammatoriese merkers (TNFα, MCP-1 ens.) in die vet gemeet.

Resultate: Vanuit die resultate verkry met die afhandel van die studie is daar geen gewigs toename opgemerk nie. In die vetweefsel van die vroulike diere is daar opmerklik kleiner selle met 'n duidelike verhoogde adiponectin vlakke waargeneem wanneer dit met sitokien vlakke in die vet weefsel van die manlike diere vergelyk word. Terselfdetyd was die pro-inflammatoriese merkers -TNFα en MCP1 – ook in die vet weefsel van die vroulike diere verhoog in vergelyking met die van die manlike diere.

Gevolgtrekking: Saamgevat wys die data gegenireer vanuit die studie dat DTG moontlik vetweefsel gesondheid negatief beinvloed. Dit stel ook voor dat die vroulike geslag meer vatbaar is vir ongewensde langtermyn uitkomste. Die kleiner vetselle wat in die vetweefsel waargeneem word is in lyn met die moontlike aandeel wat DTG het in kroniese lae-graadse inflammasie – dit maak patiente wat DTG-behandeling ontvang meer vatbaar vir comorbiditeite wat kroniese inflammasie as kenmerk het.

Acknowledgements

Firstly, I would like to thank my supervisor, Prof. Smith, for this opportunity. Thank you for believing in me when I didn't believe in myself. Your endless support, kind words and honest opinions are much appreciated. I could not have asked for a better supervisor to share this journey with.

Then, my co-supervisor Dr. Petersen-Ross. Thank you for all the behind the scenes work and your support throughout this process.

Dr. van de Vyver, thank you for always having an open door and many suggestions.

Tracey Ollewagen, your support and words of encouragement contributed more to the successful completion of this project than you would imagine.

Dalene de Swardt, CAF technician for assisting with flowcytometry.

The remainder of the triplets -Natasha and Janica – I think we made a great team. Thank you for all the support throughout the entirety of this process. This have been everything but easy on any one of us, but we shared a lot of tears and laughter in the process – memories and friendships I will forever cherish.

Then, I also want to thank each and every one in the department of clinical pharmacology.

And lastly, I would like to thank my family for supporting my wildest dreams. Thank you for being my main supporters – for enduring the hard parts and celebrating the little things. I would not have been able to make it this far without each and every one of you.

Table of contents

List of figures

List of tables

List of abbreviations and acronyms

AAG	Alpha-1-acid protein
AC	Acclimation
ACN	Acetonitrile
AMPK	AMP- activated protein kinase
ART	Antiretroviral therapy
ARV	Antiretroviral
ASC	Adipose derived stem cells
AT	Adipose tissue
ATGL	Adipose triglycerol lipase
AUC	Area under curve
BAT	Brown adipose tissue
BMI	Body mas index
C/EBPα	CCAAT/enhancer-binding protein-α
cART	Combination antiretroviral therapy
CCL	C-C motif cytokine ligand
C_{max}	Maximum plasma concentration
COL1	Collagen I
COL6	Collagen VI
CYP450	Cytochrome P450
DAMPS	Damage associated molecular patterns
DMSO	Dimethyl sulfoxide
DTG	Dolutegravir

ECM	Extracellular matrix
ETDA	Ethylenediaminetetraacetic acid
FA	Formic acid
FBS	Foetal bovine serum
FMO	Fluorescence minus one
GLUT-4	Glucose transporter 4
GM-CSF	Granulocyte-macrophage colony stimulating factor
HIF	Hypoxia-inducible factors
HIV	Human immunodeficiency virus
HPLC	High pressure liquid chromatography
HSL	Hormone sensitive lipase
IL	Interleukin
INF-γ	Interferon γ
INSTI	Integrase stand transfer inhibitor
LPS	Lipopolysaccharide
MCP-1	Monocyte chemoattractant protein1
M-CSF	Monocyte colony stimulating factor
MMP	Metalloproteinases
MSC	Mesenchymal stem cells
MPO	Myeloperoxidase
NFκB	Nuclear factor Kappa B
NSTI	Nucleoside reverse transcriptase inhibitors
OCT	Tissue freezing medium

PBS	Phosphate buffered saline
PenStrep	Penicillin/Streptomycin
PLWH	People living with HIV
PPARγ	Peroxisome proliferator-activated receptor-gamma
RNS	Reactive nitrogen species
ROS	Reactive oxygen species
SAT	Subcutaneous adipose tissue
SD	Standard deviation
SVF	Stromal vascular fraction
TGF-β	Transforming growth factor β
TIMP	Tissue inhibitors of metalloproteinases
TLR	Toll-like receptor
TNFα	Tumor necrosis factor α
UCP-1	Uncoupling protein -1
UDP	Uridine diphosphate
UGT	Glucaronosyl-transferase
UV	Ultraviolet
VAT	Visceral adipose tissue
WAT	White adipose tissue
WHO	World Health Organization

Chapter 1: Introduction

Human immunodeficiency virus (HIV) remains a prominent health problem worldwide. According to the UNSAIDS database, the number of individuals living with HIV were an estimated 30.1 – 45.1 million people in 2020.[1] This included an estimated 9.8 – 10.2 million people who were not utilising or accessing HIV treatment.[1] Despite large amounts of resources invested in HIV and antiretroviral (ARV) research, there is still much work to be done in this field to fully elucidate the effects of HIV and ARV therapy (ART). Major advances have been made since the introduction of ARVs onto the market and into the treatment regimen of people living with HIV (PLWH) infections, but intricate details regarding the longer-term effects of ARV drugs remain under-researched.

One of the main issues that obstruct advances in the mission to find a cure for HIV, or a disease management drug that is free of multiple side-effects, is the fact that latently infected immune cells (e.g. resting memory T cells and macrophages)[2–4] may affect the tissues they reside in.[4–7] Viral latency is a state of reversible non-productive infection of individual cells - which contributes an important aspect to viral persistence.[8] These cells have the potential to escape immune recognition[8] and with ART affecting various steps within the viral replication process – a process not actively taking place in latently infected cells – HIV also evades the ART action. The tissues in which these latently infected cells reside are known as viral reservoirs. The ability of HIV to establish itself in viral reservoirs together with chronic inflammation are two crucial aspects to overcome.

In terms of treatment, current ARVs are quite potent and can successfully suppress the plasma viral load to below detection threshold. However, it is hypothesised that there is limited drug penetration into some of these tissue-located viral reservoirs which results in subtherapeutic drug concentration[9], which in turn fails to reduce tissue viral load. Apart from the resulting chronic and uncontrolled viral infection, the ensuing chronic inflammation – the leading cause of morbidity amongst PLWH with ART-controlled HIV infections[10] – also increases the risk for many chronic inflammatory co-morbid conditions, as indeed observed in HIV.

Given the significant contribution of obesity to risk for chronic conditions with an inflammatory component that are common co-morbidities in HIV (e.g. cardiovascular disease and diabetes), investigation into adipose tissue (AT) health is warranted in the context of HIV and ARVs.

Of particular relevance to the current thesis, the new generation integrase strand transfer inhibitor (INSTI) and first-line ARV drug currently gaining popularity in Africa – dolutegravir (DTG) – has been linked to weight gain, hyperglycaemia and AT insulin resistance.[11–13] Although comprehensive pharmacokinetic data on DTG in AT is currently lacking, a report suggests low penetration of DTG into AT.[9] Nevertheless, even at low levels, ARV drugs may potentially have detrimental effects on tissue. Indeed, in the case of DTG, a poorer metabolic and pro-fibrotic outcome was illustrated in human adipocytes in cultures and in DTG-treated human and simian AT biopsies.[14] These effects of DTG may indicate a contribution by DTG to inflammatory processes in AT, further exacerbating the situation and thus increase the risk for co-morbidities. The side-effects of DTG mentioned above, which all link to AT, support this hypothesis.

AT is widely distributed within depots throughout the body, where it has important endocrine, paracrine and autocrine potential. [15,16] Adding to the complexity of this tissue, the metabolic- and immune- cells residing within the AT are in close proximity[17,18]. This allows for cross-talk between these cell populations in response to HIV and/or ART.

In terms of specific cellular role players in AT, the polarization of macrophages in the context of weight gain and obesity is well defined. This phenomenon is characterized as a state of chronic, low-grade, 'sterile' inflammation associated with endocrine dysregulation[19] and macrophages phenotypic shift tending to show bias towards a pro-inflammatory phenotype with increased M1 gene expression.[20–24] This results in an overall pro-inflammatory profile in AT.[17,20,25,26] Macrophage accumulation is observed when there is an increase in AT.[20] These cells in turn are a major source of inflammatory mediators (such as transcription necrosis factor-α (TNF-α), monocyte chemoattractant protein-1 (MCP-1) and Interleukin (IL)-1β)[27] which in essence, contributes to the low-grade inflammation associated with both aging and obesity.[27] This ultimately has various undesired consequences for the overall health of individuals and will likely increase the risk of numerous co-morbidities. However, even in the absence of obesity or significant weight gain, ARVs may still have undesired effects on

cellular role players in AT, such as macrophages. The observations in DTG-treated human and simian models already mentioned, supports this theory. Thus, studying the effects of DTG on AT *in vivo*, but without the confounding effects of obesity or HIV, will elucidate the risk profile of DTG in the context of AT health.

Therefore, the aim of this thesis was to elucidate in AT of DTG-treated rodents, the effects of long-term DTG treatment on inflammatory and metabolic signaling, as well as macrophage phenotype profile.

In the next section, I provide a review of the most pertinent literature.

Chapter 2: Literature review

2.1 Introduction

DTG, an INSTI, is being favored by the World Health Organization (WHO) as part of the first-line HIV treatment regimen in countries such as Sub-Saharan Africa. However, clinical evidence suggests undesired AT health outcome as a prominent phenomenon in DTG-based ARV regimens in both treatment experienced and treatment naïve patients.[14] However, the exact mechanism(s) leading to these observations remains to be fully elucidated.

In non-HIV conditions characterized by chronic inflammation, such as ageing[28] and rheumatic disease[29], chronic unresolved inflammation has been linked to dysregulation of macrophage phenotype, which ultimately results in increased fibrosis. The increased fibrosis reported in adipose of DTG-treated patients[14], therefore may suggest a role of DTG in macrophage dysregulation and chronic inflammatory activation. However, these potential mechanisms by which DTG may adversely affect adipose health, in the absence of HIV and obesity, remains to be fully elucidated. The aim of this thesis is therefore to elucidate the effects of DTG on AT, its secretome and overall inflammatory profile – including macrophage phenotype profile - to gain some insight and perspective on this fist-line drug in the absence of confounding factors such as HIV and/or obesity, which are currently limiting conclusions on the risk profile of DTG.

In this chapter, I will firstly summarise the currently available information on DTG characteristics, pharmacokinetic properties, and clinical effects. This will be followed by a comprehensive review of the role of different cellular and signaling role players in AT, as well as relevant literature on DTG in this context.

2.2 Dolutegravir: a clinical perspective

The current HIV treatment strategy, termed combination antiretroviral therapy (cART), is the use of a combination of at least three ARV agents – preferably from different ARV classes – which allows the inhibition of viral replication at various steps throughout the viral integration and/or replication process. This ultimately assists in more effective treatment and suppression of viral replication, even in the instance of drug resistance to some ARVs.[30] The current ARV drug class combination utilized as first line therapy in South Africa (according to the updated

2019 ART clinical guidelines) are two nucleoside reverse transcriptase inhibitors (NRTIs) (300mg tenofovir disoproxil fumarate and 300mg lamivudine) and an INSTI (50mg DTG).[31] DTG-based cART regimens may be prescribed to patients who meet the criteria of being i) 10 years of age or older and ii) weighing 35kg or more.[31]

Numerous studies have been conducted to assess the safety and efficacy of DTG, albeit with limited focus. Evidence suggests that DTG has equivalent and in some cases superior viral suppression capabilities compared to existing treatments in both treatment experienced and treatment naïve patients.[32] As a result, efavirenz (EVF) is being phased out and DTG recently became the preferred INSTI, forming part of the first line cART in numerous countries, including Sub-Saharan Africa.[14,33,34] The use of DTG is being favoured as it presents with high potency, low cost, few known drug-drug interactions, superior tolerability and low risk of resistance emergence.[35–37]

Despite its low risk for drug resistance, conflicting evidence was gained from studies pertaining to the use of DTG as monotherapy. One of these studies is the DOMONO trail that recommended clinicians to refrain from prescribing DTG as monotherapy, due to an increased incidence of virological failure when compared to triple therapy.[38] Similar conclusions have been drawn following a 24-week[36,39] and a more recent 48-week study.[36] In addition, it has been suggested that DTG monotherapy favoured the emergence of INSTI resistance that severely compromised the further use of this class[36], although some controversy still exist on this topic. The fact that potential mechanism(s) that may leads to virological failure during DTG monotherapy remains unclear[36], precludes firm conclusions on this matter.

Unfortunately, like most preceding ARV dugs, there are adverse effects associated with DTG treatment. It has been reported that the incidence of adverse effects in patients on DTG based regimens that leads to discontinuation of treatment, range from 2.3 – 3.7%.[40] Adverse events reported include: neuropsychiatric symptoms, diarrhoea, nausea, vomiting, fatigue, weight gain, metabolic disorders, hepatic outcome, renal outcome and gastrointestinal outcomes.[41–43] Of these adverse events, neuropsychiatric symptoms have the highest incidence.

Neuropsychiatric symptoms have been reported in all INSTIs, and generally present within weeks after commencing treatment. One of the most commonly reported symptoms are

insomnia and others include headaches, anxiety, irritability, dizziness, poor concentration, altered dreams, depression, unexplained pain, and more recently mood changes.[40,41,43] In a recent cohort study that included more than 6400 participants from different countries, the observed neuropsychiatric adverse events accounted for about 3.5% of treatment disciontinuation.[40] Although the neuropsychiatric side-effects of DTG is not directly relevant to the current thesis topic, it is of relevance to note that many of these symptoms, such as insomnia, anxiety and depression, as well as neuropsychiatric pathology in general, have dysregulated inflammation as a characteristic.[44] This, together with the fact that brain tissue contains a large component of AT (both brown and white), does provide some support for our notion that dysregulated AT signalling may be a significant mechanism responsible for many side-effects reported by/in DTG-treated patients, including at least some of the neurological outcomes.

More directly relevant to the current thesis topic, the weight gain caused by ART can generally be characterized by increased AT accumulation relative to lean weight.[45] Weight gain is a common phenomenon among PLWH on ART and have been observed in all ARV classes,[11] but INTIs presents with more significant central and peripheral weight gain in PLWH. This is a phenomenon particularly evident in both treatment-naïve and -experienced patients on DTG - and to a lesser extent raltegravir - based regimens.[14] Early in the HIV pandemic, weight gain was considered to be part of a 'return-to-health' phenomenon. Especially in individuals with low baseline body mass index (BMI), low $CD4^+$ cell counts and high HIV RNA levels. Weight gain was associated with improved survival and immunological recovery.[11,46] However, as AT health itself has not been investigated in this context, weight gain as result of metabolic and/or inflammatory dysregulation cannot be excluded.

Furthermore, especially given the increase in life expectancy of PLWH following the introduction of ARTs, the risk of, and management of comorbidities are becoming increasingly important in the long-term management of patients with controlled HIV on ART.[47] HIV-related inflammation and immune activation are well described causes of cardiometabolic comorbidities among ARV-treated PLWH.[11] In general, weight gain is associated with increased risk for various aging-related comorbidities like diabetes and cardiovascular disease.[11]

A study conducted by Bourgi et. al. [48], compared weight gain in patients treated with various ARVs. Dramatic changes were described within the first year after treatment initiation, whereafter the change became more gradual.[48] It was illustrated that weight gain was ARV drug-specific, with DTG presenting with significantly higher average-adjusted weight gain compared to the other ARVs included in the study.[48] The exact mechanism that drives weight gain in patients using DTG-based regimens remains unclear.

Numerous hypotheses on the possible effects that DTG may exhibit on factors such as energy homeostasis, appetite regulation, hyperglycaemia and insulin resistance, have been suggested in a quest to explain the side-effects of this drug. One such hypothesis is that DTG inhibits the melanocortin 4 receptor, which is associated with energy homeostasis and appetite regulation, although likely only at supratherapeutic concentrations.[49] An alternative hypothesis implicates the magnesium chelating capabilities that DTG utilises to inhibit the viral integrase enzyme.[34] Magnesium plays a critical role in glucose metabolism and insulin resistance, where it acts as an important co-factor and second messenger respectively.[34] It is thought that by chelating magnesium, DTG may interfere with glucose transport via the glucose transport-4 (GLUT-4) receptor, resulting in increased glucose synthesis by the liver.[34]

Despite the numerous clinical studies focused on hyperglycaemia and metabolic sequelae of DTG use, and despite the fact that common co-morbidities in HIV have a significant inflammatory component, there is still a relative lack of research on the effects of DTG on the inflammatory system – and even less focused on adipose health. This thesis aimed to reduce this gap in the literature. In the next section, the literature describing availability of DTG in different tissues, including adipose, is reviewed.

2.3 Dolutegravir: pharmacokinetics and tissue distribution

DTG is intended for once-daily administration without requiring co-administration of any pharmacokinetic boosters - regardless of food consumption.[30,50–54] This is supported by the long terminal half-life of the drug. The half-life of DTG differs between people with and without HIV, ranging between 11-12 hours and 13-14 hours respectively.[50] Once administered, DTG is rapidly absorbed and reaches median maximum plasma concentration (C_{max}) in 0.5 to 2.5 hours after administration.[55]

In terms of drug metabolism and clearance, in contrast to other ARVs that are predominantly metabolised by the cytochrome P450 (CYP) 3A pathway, DTG is metabolised by means of phase II metabolism - primarily hepatic glucuronidation via uridine diphosphate (UDP) glucaronosyl-transferase (UGT) 1A1.[30,56] CYP3A4 enzymes, UGT1A3 and UGT1A9 have minimal contributions towards DTG metabolism.[56,57] Subsequently, DTG is mainly excreted in faecal matter, whereas its metabolites are excreted in urine.[55]

DTG is highly protein bound, with a fraction of >99% bound to albumin and alpha-1-acid protein (AAG).[7,32,58] This was observed in various species including rats, monkeys and humans.[59] The highly protein bound nature of DTG is one of the characteristics thought to impact the tissue distribution of the compound.[7] In general, there are contradictory insights pertaining to the tissue distribution of DTG. It is thought that DTG has good tissue penetration and that it retains the ability to cross the blood brain barrier.[60] This is supported by the fact that DTG has been detected in various bodily fluids which includes the cerebrospinal fluid. However, the degree of tissue exposure to various ARVs was illustrated in a murine model to be drug and tissue specific, with DTG levels exhibiting very little variability between tissues, with the exception of the brain – a major viral sanctuary – where ARV exposure levels were below those of other tissues.[9] Interestingly, none of the concentrations detected within the various tissue (which included the liver, AT, digestive tract, pancreas, spleen, lymph nodes and colon) were above the corresponding inhibitory concentration. From this study, it was concluded that DTG has generally low tissue penetration capacity. All tissues analysed also exhibited lower levels of DTG when compared to plasma concentrations, a feature that was more pronounced in the DTG-treated animals when compared to animals treated with the other two ARVs studied.

To date, the tissue distribution of many other ARV classes have been studied but information regarding the tissue distribution of DTG remains sparse.[61] In a real-life cohort study, the average volume of distribution of DTG was reported as 14.6L, with factors like body weight and smoking having an impact.[62] The distribution of DTG in AT specifically remains to be fully elucidated. Nevertheless, since several adverse effects of DTG on adipocytes and AT have been reported from *in vitro* studies (refer to section 2.5 below), an investigation in an *in vivo* model may shed more light on whether *in vitro* risk translates into an *in vivo* situation, given

the reported low penetration of DTG and the limitations of *in vitro* study design, where assumptions on tissue penetration and absorption are often overestimations.

2.4 Adipose tissue

AT is made up of two distinct cell fractions, surrounded by extracellular matrix (ECM).[18] The main cell fraction is lipid-laden mature adipocytes, which constitutes about 60% of the total cell population, and the stromal vascular fraction (SVF), a heterogenous cell population constituting the remainder of the cell population.[63] The composition of the SVF is highly dependent on the surrounding microenvironment and the nutritional status of the individual.[16] Cells that contribute to this cell fraction are preadipocytes, endothelial cells, fibroblasts and immune cells.[18,64] T cells and macrophages make up the majority of immune cells in AT, but essentially all types of innate and adaptive immune cell can reside in AT of both human and rodents – at least transiently - depending on disease states or presence of potential immunological challenges.[18] These cells constantly communicate with adipocytes to allow for maintenance of AT function.[63] The surrounding ECM is made up of a variety of both fibrillar (I and III) and non-fibrillar (IV, VI and VIII) collagens, laminins, fibronectin and proteoglycans. The ECM will be discussed in more detail in the unresolved inflammation section. (Section: 2.5)

2.4.1 General adipose tissue structure and cellular content

AT is quite diverse and serves to fulfil numerous functions, including energy storage and release, fatty acid handling, various endocrine and immunomodulatory functions, protection of vital organs and thermoregulation.[16,65–67] There are three distinct AT lineages, each differing with regard to their metabolic activity, location, plasticity, vascularization and innervation.[63] The different types of AT includes white, brown, and beige AT.[65,67–69] Another phenotype, namely pink adipocytes, was identified as a female specific cell type that arises from subcutaneous AT depots during pregnancy. [70]

Brown AT (BAT) is characterized by high mitochondrial content, a large number of small intracellular lipid droplets and the expression of high levels of uncoupling protein 1

(UCP1).[69,71,72] BAT mainly presents with unique thermoregulatory capacity and is the dominant site of non-shivering thermogenesis in both rodent and infants.[25] It has been illustrated to persist in adult humans, where it is preferentially located in the cervical, supraclavicular, mediastinal, paravertebral, suprarenal and perennial regions.[25] Another type, beige (also 'brite' or 'inducible brown') AT , has intermediate morphology between that of white- and brown- AT.[73] One main differences between brown- and beige AT is that BAT is found in distinct depots throughout the body whereas beige adipose can most notably be found within subcutaneous adipose tissue (SAT) depots.[71] The factor that contributes to the uniqueness of the adipocytes found in these depots, is that it can either be thermogenic or present with a predominant storage phenotype depending on environmental condition.[73] Both brown and beige-AT have been reported to protect against obesity and associated metabolic disorders – such as hyperglycemia. However, although these adipose types seem less susceptible to inflammatory stimuli in an acute situation, they too show impairment in a chronic scenario which appears representative of inflammation and metabolic dysregulation similar to the profile seen in white adipose tissue (WAT).[74] Thus, adipose type seems to be less relevant in the current context of HIV and long-term DTG use. Therefore, I will focus on WAT from here on, for which more information is available in the context of ART.

WAT depots are distributed thought the entirety of the body and its exact function is highly dependent on where it is located.[63,75] Different depots are highly heterogenous and present with various physical, physiological and precursor population differences.[76] The two main depots into which AT is distributed, are the subcutaneous- and the visceral- AT. Visceral AT (VAT) is intra-abdominal AT mainly located around organs[77] and generally displays a more pro-inflammatory profile and higher secretory capacity.[78] This higher metabolically active state has resulted in an increase in or excess of VAT, which is considered a major risk factor for chronic diseases such as cardiovascular and metabolic conditions, independent of general adiposity.[79] Some of the metabolic conditions include hypertension, type II diabetes, hypercholesterolemia, hypertriglyceridemia and metabolic syndrome, as well as other health complications. SAT is mainly found under the skin where it aids in thermoregulation, serves as cushioning and acts as a barrier against dermal infection. SAT plays a less significant role in chronic inflammatory or metabolic disease.[78] In clinical research however, SAT is more commonly evaluated than VAT, likely due to ease of access. Thus, clinical data on ARV effects on AT may not accurately reflect the metabolic effects at a VAT level. In this context,

10

an *in vivo* rodent model – where VAT can be accessed with relative ease at the end of a protocol – may provide more accurate information.

In terms of specific signalling, WAT tissue exhibits important endocrine, paracrine and autocrine potential [15,16] and is recognized as a central metabolic, regulatory organ. WAT exerts its effects via synthesis and release of various biologically active compounds which will be collectively referred to as adipokines for the purpose of this review.[63,67,73,80] These adipokines can be characterised as either pro- or anti-inflammatory and participate in both local and systemic inflammatory processes.[45,81] Adipokines are made up of true adipokines, mainly secreted by the AT, and cytokines secreted by both the immune cells in the SVF and the adipocytes.[81] The key to healthy AT seems to be the maintenance of a balance between the pro- and anti-inflammatory adipokines.[20] This balance is dependent on numerous factors such as nutritional/metabolic status of the host, the presence of infection or systemic inflammation, oxidative stress, cigarette smoke exposure, age and sex – and potentially drugs such as DTG. [81] Circulating levels of adipokines are affected by changes in overall adiposity, the anatomic distribution of fat depots, adipocytes size and lipid content, and the composition of AT immune cell populations.[45] Anti-inflammatory dysregulation or inadequacy, caused by factors such as AT accumulation, results in a relatively more pro-inflammatory shift. Similarly, in obesity, infiltrated macrophages have been illustrated to increase pro-inflammatory bias in AT. The end result is an unhealthy tissue characterised by elevated secretion of pro-inflammatory adipokines (TNF-α, IL-6, leptin, resistin) and reduced secretion of the anti-inflammatory ones (e.g. adiponectin).[20]

At this point, it is perhaps pertinent to point out a significant consideration in terms of adipose-related research. There are major sex differences in body fat distribution in humans and other mammals.[82] When considering females, AT is predominantly distributed subcutaneously in the gluteal-femoral or peripheral regions, giving rise to a "pear shape" figure. This pattern of fat distribution is associated with lower metabolic risk and can potentially even be protective against adverse health effects associated with obesity in both males and females, although this does not mean that females cannot present with an upper-body obese phenotype.[83] On the other hand, central or abdominal fat deposition, especially deposits in the VAT depots surrounding vital organs, increase an individual's risk of developing metabolic complications. This phenotype is most commonly seen in males and is known as an "apple shape" or so

called android distribution.[82,84] The higher levels of visceral adiposity are associated with higher levels of postprandial insulin, fatty acids, and triglycerides and increased risk for cardiometabolic conditions. [83] It is therefore imperative to include both sexes in research related to AT health.

In further support of this, adiponectin indeed also presents with sex-specific trends, with higher levels secreted in females than males. Moreover, studies also demonstrated a depot-specific trend, with higher levels detected in subcutaneous AT depots compared to the visceral AT depots.[80] Factors that increase circulating adiponectin levels include calorie restriction, aging, estrogen deficiency, Type I diabetes, and treatment with thiazolidinediones, whereas the contrary is true for obesity, Type II diabetes, oxidative stress, and cigarette smoke exposure. [80] Adiponectin levels in obese individuals are one of the key features that differentiate metabolically healthy obese individuals from metabolically unhealthy individuals[45] and is thus a key biomarker to include in evaluations of adipose health profile.

2.4.2 Specific cellular role players in adipose tissue

The following section will give some insight on the cellular role players in AT and the specific contributions each have toward the net inflammatory status of AT. Although all relevant cell populations in AT will be included, I will place specific focus on adipocytes and macrophages, as major role players in adipose health.

2.4.2.1 Adipocytes

Adipocytes within the WAT are characterized by a single large intracellular lipid droplet with a flattened peripheral nucleus.[63,73] It is the primary site for lipid storage and lipid mobilization. In addition, it plays an important role in the regulation of energy homeostasis in response to nutrient surplus or demand. [67,73,75] During periods of nutrient depravation, the body will sense a decrease in blood glucose levels. Consequently hormones such as glucagon and noradrenaline will be released which will stimulate adipocytes and activate enzymes such as hormone sensitive lipase (HSL) and adipose triglycerol lipase (ATGL). These hormones and

enzymes result in the release of non-esterified fatty acids and glycerol from the lipid droplets into circulation for organs to utilise.[71,80] In contrast, during times of nutrient excess, the blood glucose levels rise, resulting in insulin secretion, which in turn suppresses HSL and ATGL. In addition, promoting the upregulation of *de novo* lipogenesis to package lipids into droplets for storage of the excess nutrients. Increasing evidence further suggests a role for adipocytes in other aspects of systemic metabolic homeostasis.[80,85] For example, it also protects tissue from toxic lipid accumulation (lipotoxicity) by sequestering excess lipids and storing it within a large lipid droplet within the cell.[71] The large lipid droplet is packed with products of esterified free fatty acids and triglycerides (the from in which excess energy is stored).[69,71,72]

2.4.2.2 Stromal vascular fraction

The AT SVF is a versatile, heterogenous and clinically relevant cell system.[86] The SVF is known to be composed of a variety of cells that include fibroblasts, mesenchymal stem cells, endothelial cells, smooth muscle cells, mural cells and immune cells.[86] Infiltrating immune cells (e.g. macrophages, B cells and T cells) are the second largest cell population that is found within AT. These cells play a critical role in regulating tissue function and maintaining tissue homeostasis. [85]

At this point, the composition of the SVF is well studied but unanimity has not yet been reached with regards to the specific proportion that each constituent contributes.[86] The composition of the SVF is highly variable and depends on factors such as the site of adipose isolation, the processing methods used, and the patient's overall health and pathological conditions.[86]

2.4.2.3 Macrophages

Macrophage development occurs during both early foetal development and adult life. [87] In early life stages these cells are most commonly derived from the yolk sac and foetal liver. [87,88] These organs are responsible for generating the heterogenous long-lived tissue resident macrophages that are widely distributed in different organs and tissue with diverse functions

13

and subsets.[87] As the life stages progress, macrophages are derived from bone marrow stem cells in response to monocyte colony stimulating factor (M-CSF) to form monocytes (the precursor of macrophages), circulating in the blood.[89] Once an inflammatory response is initiated in the body, these monocytes migrate to the site of inflammation where they mature to macrophages and perform their functions. These functions range from phagocytic and pro-inflammatory effects, to anti-inflammatory, inflammation resolving and tissue remodelling signalling.[89–91]

Macrophages are highly plastic, versatile and heterogenous cells found in all tissues with phenotype and function dependent on the surrounding microenvironment.[16,66,92–94] Initially, macrophage phenotypes were thought to simple. It was proposed that macrophages could be classified using only the M1/M2 paradigm. However, it is now known that there are more subtypes, each of which can be characterised based on expressed markers and cytokine secretions, in combination with phagocytic and antigen-presenting functions.[88,95] Importantly, macrophage phenotypes do not represent different and fixed subpopulations of macrophages – rather, that a macrophage can switch from one to another phenotype, in a manner dependent on its cytokine environment, which facilitates polarisation at transcriptional and post-transcriptional levels.[96] In addition, there are alterations to cellular metabolism that accompany the shift in phenotype.[91] M1 macrophages seem mainly dependent on glycolysis whereas M2 macrophages rely mainly on oxidative phosphorylation.[91]

The M1 phenotype is known to be generally pro-inflammatory and arises in response to signalling by interferon (IFN) -γ, TNF-α, granulocyte-macrophage colony stimulating factor (GM-CSF), lipopolysaccharide (LPS) and other endotoxins.[29,97,98] M1 macrophages promote inflammation by producing/secreting pro-inflammatory mediators such as IL-6, IL-12, IL-23, TNF-α, MCP-1 and IL-1β,[29,99] and plays a major role in the removal of necrotic material via phagocytosis. These cells also take part in processing and presenting antigens which results in the activation of T-cells.[97]

The M2 macrophage population is more complex and exists in a continuum of various subtypes, denoted by a, b, c and d.[29] The M2d phenotype is largely associated with angiogenesis in tumor growth and is not necessarily relevant to the current topic – for this reason only M2a, b and c will be discussed. M2a macrophages will result from IL-4 and IL-13 exposure and its secretome is still largely pro-inflammatory. This phenotype contributes to

tissue repair, wound healing and fibrosis.[29,98] When the tissue damage (or other pro-inflammatory stimulus) has been cleared via the action of M1 and M2a macrophages, the secretion of pro-inflammatory cytokines will decrease, changing the cytokine profile to a relatively anti-inflammatory inducing one (containing transforming growth factor (TGF) -β and IL-10). This cytokine landscape directs the phenotype switch of M2a to M2c macrophages. These cells in turn secrete more IL-10 and TGF-β, as well as C-C motif cytokine ligand (CCL) -16 and -18 and contributes to resolution of inflammation and limitation of fibrosis. However, in a scenario where the pro-inflammatory trigger is chronic (e.g. due to the self-propagating cycle of inflammation and oxidative damage) and toll-like receptor (TLR) activation in combination with IL-1β levels remain elevated, this phenotype switch is incomplete. This results in macrophages appearing "stuck" in an intermediate phenotype – the M2b.[29] This phenotype retains the capability of secreting pro-inflammatory cytokines, but in addition to also acquiring the capacity to release anti-inflammatory cytokines. As result, the cytokine profile in the intercellular environment becomes hugely dysregulated, perpetuating a chronic, unresolved inflammatory condition characterised by tissue dysfunction/damage and significant fibrosis.[29]

2.4.3 Adipose tissue signalling

The following table represents potential biomarkers to distinguish between a pro- and anti-inflammatory profile within the AT. This includes IL-10, MCP-1, IL-1β, TNFα, adiponectin and resistin. It also states the main source of the various adipokines, on the trends previously observed in ARV context. **Table 2.1: adipose tissue signaling.**

Secretory products	Cells	Pro-/anti-inflammatory net effect	Adipokine in ARV context
Adiponectin	Adipocytes [100]	Anti-inflammatory, anti-fibrotic and antioxidant effects [100]	DTG reduce secretion [101,102]
IL -10	Secreted by immune cells including macrophages, dendritic cells, B- and T- cells.[22,103]	Anti-inflammatory cytokine[22] Anti-inflammation, inhibition of the pro-inflammatory cytokines[103]	
IL-1β	Macrophages and monocytes[103]	Pro-inflammatory, proliferation, apoptosis, and differentiation	
Resistin	Macrophages, monocytes, neutrophils [81,104] (In rodents it is secreted by adipocytes)	Induces secretion of other pro-inflammatory cytokines like TNF alpha, IL-1Beta, IL-6, IL-8 and IL-12 [105] Promotes the expression of adhesion molecules which includes MCP-1[106]	
TNF-α	Mainly secreted by monocytes/macrophages[107] NK-cells, CD4+ lymphocytes and adipocytes	Prototypic inflammatory cytokine and neutrophil chemoattractant [107] Pro-inflammation, cytokine production, cell proliferation, apoptosis , anti-infaction[103]	
MCP-1	Epithelial cells, endothelial cells, smooth muscle cells, monocytes/macrophages, fibroblasts, astrocytes, mesangial and microglial cells [107,108]	Pro-inflammatory[22], plays a role in the chemotaxis of monocytes and is associated with increased oxidative stress.[108]	Decrease in MCP-1 expression[102]

16

2.5 Unresolved inflammation and related consequences

As previously mentioned, AT is a complex organ that takes part in major regulatory functions. As a result of the complexity and intricate role that this tissue plays – it has the ability to rapidly and dynamically remodel in response to the metabolic environment.[109] AT remodelling – is the term used to describe the changes that occur in the AT as it adapts to its everchanging surroundings – is modulated by an inflammatory response orchestrated by various immune cells, which includes macrophages and lymphocytes.[110]

Inflammation acts as a vital defense mechanism. It is not only crucial for health but also plays an important role in the pathogenesis of many chronic diseases like cardiovascular disease, bowel diseases, diabetes, arthritis, and cancer. Inflammation is the body's physiological response to infectious or non-infectious insults like pathogens, cell damage, noxious compounds, and irradiation.[103] The inflammatory response acts by removing/eliminating the harmful stimulus – ultimately initiating tissue healing and restoring tissue homeostasis.[103] The initiation of an inflammatory response orchestrates numerous consequences in the surrounding microenvironment which includes vasodilation, increased blood flow and increased vascular permeability, allowing short-lived neutrophil infiltration and accumulation in surrounding tissue.[89] The neutrophils are later replaced by lymphocytes and macrophages that are responsible for secreting growth factors, cytokines and other inflammatory mediators.[89,103] Although this is the consequence of tissue injury and wound healing, similar inflammatory responses have been illustrated in response to the damage associated molecular patterns (DAMPs) expressed during adipocyte death.[111,112] The body's response to one or more of these insults are considered to result in an self-limiting acute inflammatory response, but if left unresolved, results in a state of chronic inflammation.

Chronic inflammation is one of the leading causes of eventual morbidity and mortality worldwide.[113] The concept of chronic low-grade inflammation within AT has been well described in the context of obesity and is one of the contributing factors that lead to AT dysfunction.[27,114,115] Other key role players that take part in AT dysfunction are fibrosis and hypoxia that result from maladapted angiogenesis and exacerbated tissue expansion.

The expansion of AT can be facilitated by means of two mechanisms namely adipocytes hypertrophy (increased cell size) and the more metabolically favourable adipocyte hyperplasia (increased cell number).[69,71,72,80] Adipocytes that have undergone hypertrophy – a known stressor for adipocytes [116]- have been illustrated to exhibit numerous necrotic-like abnormalities such as ruptured plasma membranes, endoplasmic reticulum stress, cellular debris in the extracellular space, and presence of small lipid droplets in the cellular cytoplasm.[24,69] These enlarged cells have also been associated with free fatty acid fluxes, hypoxia, adipocyte death and increased pro-inflammatory cytokine (leptin, IL-8, IL-10 and MCP-1)[117] production and release - resulting in increased immune cell infiltration and recruitment [24,110] – a chain of events that synergistically leads to creating a pro-inflammatory microenvironment within the AT.[72] This creates a vicious loop that continuously feeds itself. The pro-inflammatory micro-environment results in increased immune cell infiltration that will continue to produce pro-inflammatory cytokines and thus recruit more immune cells. In turn, this will supress secretion of insulin sensitising adipokines like adiponectin and IL-10. The release of pro-inflammatory cytokines also contributes to insulin resistance by activating Nuclear factor Kappa B (NFκB) and Jun-N terminal kinase signalling pathways, which results in the serine phosphorylation of insulin receptor substrate-1.[110]

A key contributor to insulin resistance and a factor closely associated with chronic inflammation is oxidative stress – although consensus has not yet been reached on whether chronic inflammation or oxidative stress occur first, these two factors are fuel to the other's fire. Oxidative stress is the consequence of the body's antioxidant capacity being outweighed by the overproduction of oxidants. Oxidants are products of normal physiological responses and cellular metabolism commonly referred to as reactive oxygen species (ROS).[118–120] The resident and recruited macrophages and neutrophils are responsible for clearing cellular debris of dead and/or dying cells and in turn produce ROS and reactive nitrogen species (RNS). ROS takes part in important regulatory roles in AT biology. When the balance between pro-oxidants and antioxidants no longer exists, ROS accumulation occurs which – among other things – results in insulin resistance. Insulin resistance is often associated with cardiovascular disease and negative metabolic outcome.[121] In addition, ROS accumulation results in tissue damage consequently promoting fibrosis.

Furthermore, and relevant to the topic of redox dysregulation, lipid accumulation in hypertrophic adipocytes results in notable cell expansion – to such an extent the oxygen diffusion limit is reached– ultimately inducing hypoxia. As a result, stress signals are induced in an attempt to promote angiogenesis and ECM remodeling, in order to alleviate the oxygen shortage.[122] Hypoxia-inducible factors (HIFs) are the master regulars of this adaptive response.[123] Obesity-induced AT expansion has been associated with hypoxia that locally induces HIFα secretion. Apart from the insulin resistance already mentioned, the activation of HIFα has also been implicated in proangiogenic conditions in adipocytes, as well as a collagen-driven profibrotic response that resulted in maladaptive AT remodeling, where HIF1α is thought to play a role in maladaptive collagen cross linking and stabilization.[24]

Adipocyte hypertrophy, the associated hypoxia and resulting chronic inflammation and oxidative stress are all factors that contribute to AT dysfunction and dysregulation in ECM remodeling resulting in AT fibrosis. ECM remodeling forms part of the physiological process to adapt to normal AT size fluctuation.[122] In order to allow for optimal physiological functioning of the cellular contributors within AT, appropriate adipose ECM composition and remodeling plays a crucial role in maintaining the balance between ECM deposition and ECM degradation. The degradation of ECM components is driven by proteolytic enzymes - matrix metalloproteinases (MMPs).[114] In AT MMPs are secreted by a variety of cells which include macrophages, endothelial cells and fibroblasts. Tissue inhibitors of metalloproteinases (TIMPs) contributes to this tightly regulated process by inhibiting MMP activty.[122] It has been illustrated that various adipokines associated with obesity and hypoxia induce TIMP activity and concentrations in circulation. [124]

In healthy individuals a balance exists between MMP and TIMP activity – once dysregulation has occurred, generally brought about by inflammation – the rate of ECM production exceeds that rate at which ECM is degraded, resulting in excess ECM deposition and ultimately tissue fibrosis.[122] This limits the plasticity of the AT, altering AT function. Fibrosis is considered a pathophysiological consequence of the persistent low-grade inflammation in WAT in obesity [72,125] and a characteristic of AT dysfunction.[111]

The ECM in AT is made up of a wide variety of ECM components. The main contributor to AT ECM is collagen and here it provides more than just structural support.[125] Collagens take part in cell adhesion, migration, differentiation, morphogenesis and wound healing. AT fibrosis is

associated with considerable accumulation of collagen I (COL1) and collagen VI (COL6).[126] COL1 is produced by fibroblasts and is known to provide structural scaffold for cell attachment as well as, be a potent angiogenic factor.

Collagen VI (COL6) is an abundant WAT ECM constituent that accumulates in diet-induced obesity and is an important indicator of metabolic dysregulation.[127] A study conducted in a COL6 knockout model illustrated ECM destabilization resulting in decreased AT fibrosis. They demonstrated that animals on high fat diet or with *ob/ob* background had improved insulin sensitivity.[128] Decreased COL6 is associated with decreased necrosis and macrophage infiltration.[24] COL6 is an oligomer consisting of three α-chains (α1, α2 and α3) - post translational proteolytic cleavage of the carboxyl-terminal C5 domain of the α3 chain from the parental COL6 microfibril by MMPs yields an end-product called endotrophin.[127,129] Endotrophin has been illustrated to induce inflammation and stimulate fibrosis by activating the TGF-β pathway and recruiting macrophages and endothelial cells.[24] Although a wide variety of cells take part in this process it has been illustrated that macrophages exhibit critical regulatory activity at all stages of repair and fibrosis. This is because macrophages are an important source of chemokines, MMPs, and other inflammatory mediators that drive initial cellular responses in injury.[112] The M2 phenotypic subtypes – particularly M2a and M2b – plays a role in wound healing and tissue repair. These two subtypes secrete TFG-β that stimulates fibrosis and inhibits the AMP-activate protein kinase (AMPK) pathway.[24]

The cytokine profile also plays a major role in fibrosis – adiponectin – one of the prominent adipokines secreted by the adipocytes in the AT inhibit the NFκB signaling pathway, upregulates the AMPK pathway and has a potent antifibrotic effect on cultured fibroblasts.[24] Although it is produced and secreted by the adipocytes – adiponectin has an inverse relationship with adiposity. With increased AT there is decreased levels of adiponectin.

This concludes the outline of the basic physiological processes and contributors to AT dysfunction and fibrosis. This will allow better understanding of the role that DTG plays and its potential contribution towards AT dysfunction discussed in the following section.

2.6 Adipose tissue dysfunction in the context of dolutegravir

Although literature on the effects of DTG in human AT is sparse, circumstantial evidence is mounting, implicating DTG in modulation of adipose health, although results are somewhat conflicting. The following table represents various studies conducted using DTG or DTG based regimens and the most prominent observations made. (Table 2.2)

Table 2.2: summary of previous studies. The following table summarises various studies that investigated the effects of DTG on adipose- and other tissue and cell lines with an outline of the main findings.

	Model	Sex	Infectious	Mono- / combination therapy	Effects observed
Gorwood et. al. (2020)[14]	Cynomolgus Macaques (SAT and VAT)	M	Non-infected, treated for 2 weeks with INSTI containing regimen and non-treated controls.	**Combination therapy.** 20mg/kg orally / 2.5 mg/kg subcutaneously	- Fibrotic bundles and thickenings visible. - Clusters of larger adipocytes – suggested hypertrophy
	Human	M/F	Obese PLWH treated or not-treated with INTI-containing regimen.	**Combination therapy.**	- Increased fibrosis
	Human (ASCs isolated from SAT)	F	Obese PLWH treated or not-treated with INTI-containing regimen.	**Combination therapy.** DTG (3.1 µg/mL)	- Elevated levels of collagens, fibronectin, and myofibroblast markers αSMA. Suggesting increased fibrosis by promoting profibrotic phenotype in ASCs and adipocytes. - Increased ROS production and induced mitochondrial dysfunction characterized by increased mitochondrial mass a decreased membrane potential. - Decreased expression and/or secretion of adiponectin and leptin. - Lipid accumulation in differentiated, matured adipocytes

21

Ayissi et.al. (2022)[126]	Cynomolgus macaques		SIV infected and treated compared to uninfected untreated	**Combination therapy** – DTG (20mg/kg)	- Elevated PARRγ expression in VAT and SAT
	Human (ASCs isolated from SAT)		Uninfected	**Combination therapy** – DTG (3.1 µg/mL)	- Pro-adipogenic, pro-lipogenic, increased ROS production, increased collagen, and pro-fibrotic mediator expression
Bade et.al. (2021)	THP-1[130]		Uninfected	**DTG monotherapy** (0.41938 µg/mL, 4.1938 µg/mL, and 41.938 µg/mL)	- Broad spectrum MMP inhibitor
Domingo et.al. (2020)[102]	Human Simpson Golabi Behmal Syndrome adipose cells		Uninfected	**DTG monotherapy** (0.041938, µg/mL, 0.41938 µg/mL, 4.1938 µg/mL)	- No effects on morphology or adipogenesis and pro-inflammatory cytokines. - Significant decreased in MCP-1 expression. - Reduced adiponectin expression in a dose dependent manner.
Jung et. al. (2022)[131]	Mice	F	Uninfected	**DTG monotherapy** - 10mg/kg/day DTG, 5% dimethyl sulphone, 30% polyethylene glycol, 10% tween80, 55% double distilled water for 2 weeks administered subcutaneous.	- Increase in fat mass. - Reduced UCP-1 but upregulated SREBP – a master regulator in lipid synthesis in inguinal WAT. - Increased lipid accumulation in white adipocytes - Differential effects on different AT types.
Rizzardo et. al. (2019)[132]	Human	M/F	Infected	**DTG monotherapy** – 50 mg/day	- Weight gain observed – more pronounced in women.

*ASC – adipose derived stem cells

The above-mentioned table (table 2.2) illustrates the various studies conducted in order to better understand DTG and its potential effects. From this it is evident that there are conflicting views regarding the effects that DTG has on AT as well as other tissues and cell lines.

It is apparent that most of the studies reported poorer outcomes when DTG was administered in combination with other ARVs and/or with the presence of HIV /SIV infection. In these studies, it was reported that AT (both SAT and VAT) illustrated pro-fibrotic phenotypes, significant weight gain with evident adipocyte hypertrophy [14,126,131] – all of which is thought to contribute to poorer metabolic outcome.

In the studies where DTG monotherapy was administered – in the presence of HIV infection – weight gain was also reported. HIV and associated viral protein are known to alter AT homeostasis and contribute to chronic low-grade inflammation *in vivo* and *in vitro*.[10,101] AT of SIV infected, untreated macaques previously illustrated heterogenous cell sizes that ranged between small and medium-cells with the presence of fibrotic bundles.[101] The AT also illustrated decreased peroxisome proliferator-activated receptor γ (PPARγ) expression at both mRNA and protein level.[101] A later study suggested increased PPARγ expression in the SAT and VAT of infected macaques treated with cART containing DTG. Although the DTG is administered in combination with other ARVs - this suggests a possible positive prognostic outcome as PPARγ is a central role player in adipogenesis and maintaining mature adipocyte function.[133,134] PPARγ is also an important regulator in macrophage polarization, where PPARγ activation drives the alternative M2 macrophage phenotype – associated with increase secretion of anti-inflammatory cytokines and inhibition of pro-inflammatory cytokines. This likely also supports the notion to avoid DTG monotherapy as it is promoting an ant-inflammatory milieu – dampening the inflammatory response lodged against viral infection / infected cells.

Some studies support the pro-fibrotic potential of DTG , suggesting DTG acts as a broad spectrum MMP inhibitor, mainly affecting MMP-2 , -8, -9 and – 14 *in vitro*.[130] MMP-9 in particular is one of the main MMPs responsible for COL1 degradation.[135] Down-regulation of MMPs would lead to downregulated COL1 degradation and ultimately, if the inhibition of MMP9 is sustained for an extended period of time, will result in COL1 accumulation. This would result from COL1 not being sufficiently broken down. However, this study was

conducted in the THP-1 cell line - an immortalized monocyte-like cell line and might not have been an accurate representation of the effects that DTG has on monocytes or macrophages *in vivo.*

An *in vitro* study treating Human Simpson Golabi Behmal Syndrome adipose cells a with human equivalent dose of DTG illustrated no effects on pro-inflammatory cytokines, adipocyte morphology or adipogenesis with a significant decrease in MCP-1 secretion and dose dependent decline in adiponectin secretion.[102] Similarly reduced adiponectin secretion was observed in human ASCs treated with DTG-containing cART.[14]

In summary, AT is a complex structure that participates in numerous physiological functions and processes. Alterations to AT homeostasis has detrimental consequences to the health of individuals. HIV infection itself contributes to AT dysfunction and alterations. For this reason, it is necessary to elucidate the effects that DTG has on AT without the confounders of HIV, combination therapy or obesity to fully understand the effects that it may have on AT, AT health and homeostasis.

2.7 Hypothesis statement

We hypothesised that chronic DTG administration without the confounders of HIV and other ART may negatively affect AT health by favouring a pro-inflammatory cytokine profile. Given the known sex-differences that exist in terms of AT distribution, we further hypothesised that these effects of DTG may be different in males vs. females.

2.8 Aims and objectives
Aim

We therefore aimed to investigate the effects of chronic DTG administration in male and female rats, in terms of AT general health and inflammatory profile.

Objectives

In order to achieve these aims, we formulated the following objectives:

- To execute a 12-week DTG administration protocol in male and female Wistar rats
- To determine the effects of chronic DTG administration in terms of total body mass and retroperitoneal AT mass.
- To evaluate potential for DTG-associated changes in plasma and AT cytokine and chemokine profile (adiponectin, resistin, MCP-1, TNFα, IL-1β and IL-10) using commercially available ELISA kits.
- To perform a basic histological investigation to describe AT in terms of general tissue structure and adipocyte morphology, macrophage subpopulation distribution and level of fibrosis, in placebo and DTG-administered rats.

Chapter 3: Methodology

3.1 Ethical considerations and experimental animals

Following ethical clearance of all protocols by the Stellenbosch University Animal Research Ethics Committee (reference # SU-ACU-2035-2022, refer to appendix 1), 12 male and 12 female Wistar rats were obtained from the Stellenbosch University small laboratory animal breeding facility. At 7 weeks of age, these rats were divided into two experimental groups (6 males and 6 females per group), namely control and DTG-treated. The rats were housed in groups of 3 per cage in a temperature- and humidity-controlled room (23±1°C, 40-60% humidity) with a set 12h light-dark cycle (lights on at 7am). The rats had access to food (autoclaved standard rat chow) and tap water *ad libitum*. All experimental procedures were conducted according to the ethical guidelines and principles of the declaration of Helsinki.

3.2 Dolutegravir preparation

Give the extremely high cost of purified DTG, DTG was extracted and purified from commercially available tablets (Olegra®). A liquid-liquid extraction previously established in our laboratory was utilised.

Multiple extractions were performed to obtain sufficient amounts of DTG to supplement animals for the course of the 12-week study. For each extraction, two Olegra® tablets with a 50mg DTG content were used. The tablets were crushed using a glass mortar and pestle until a fine powder consistency was reached, before transferring it to a 50mL microcentrifuge tube. A volume of 10mL Milli-Q water (purified using Synergy® water purification system) was added to the powder. The water-powder mixture was vortexed for 2 minutes and then subjected to a 10-minute sonication step. 30mL Ethyl acetate was added to the water-powder mixture. The vortex and sonication steps were repeated, followed by 10 minutes centrifugation at 2000 x *g*. The resulting supernatant was transferred to pre-weighed borosilicate glass tubes and evaporated under vacuum utilising the Genevac miVac Duo Sample Concentrator at 30°C until completely dry. The powder residue that remained – the extracted DTG – in the borosilicate glass tubes was weighed and transferred to glass vials for storage and kept at 4°C in a desiccator until use. The extracted DTG were pooled to ensure consistency throughout.

Although I did not perform the extraction of DTG independently, the purity of the extracted DTG was determined by high pressure liquid chromatography (HPLC) analysis, as part of another MSc thesis. Briefly, extracted DTG was dissolved in acetonitrile (ACN) resulting in a stock solution with a concentration of 10µg/mL. The analysis was performed on an Agilent Technologies 1100 Series system (California, US) consisting of Agilent 1260 Infinity binary pumps coupled to an Agilent Series 1100 autosampler, column compartment and variable wavelength detector. Ultraviolet (UV) detection was set at 256nm and a Venusil C18 column (4.6 x 150mm, 5µm particle size) column was used for separation. Mobile phase A consisted of Milli-Q water (purified using Synergy® water purification system) 0.1% formic acid (FA) and mobile phase B were ACN, 0.1% FA at a flow rate of 0.5mL/min. The run was performed in isocratic mode (65% mobile phase B over 7 minutes) with DTG eluting at 4.85 minutes. Data acquisition and analysis was performed using OpenLab CDS Chemstation edition. The purity was determined by running a blank ACN sample, followed by a 5 µL injection of the extracted DTG sample. Any peaks present in the sample that were not in the blank were integrated and subtracted from the analyte peak area at 4.85 minutes. The remaining peak area represented the purity of the sample.
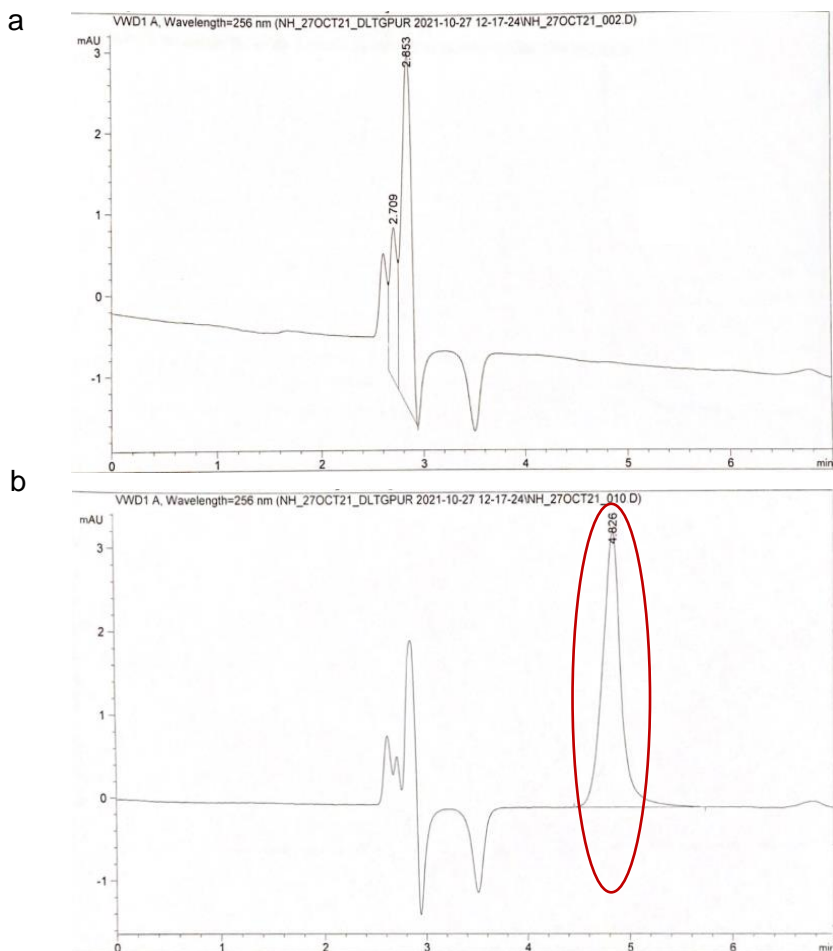

27

Figure 3.1: HPLC purity analysis. *(a) Chromatogram of blank, (b) Chromatogram and area analysis of extracted DTG sample.*

As seen in figure 3.1, there are a variety of peaks present between 2 - 4 minutes. The peaks represent the solvent front and should be the same in every sample analysed. In figure 3 B, the peak circled represents the detectors response for DTG. Due to no other peaks being present, the sample has no contamination and other compounds present at the evaluated wavelength. (Refer to appendix 3, table A for a summary of the purity analysis)

3.3 Drug intervention

Purified DTG was set in jelly blocks to allow for treatment administration. Jelly was prepared fresh each day by adding 16g dessert jelly and 0.810g gelatine to 30mL hot water. The mixture was mechanically stirred at a moderate speed until completely dissolved using flea and a magnetic stirrer. The jelly preparation was allowed to cool to room temperature. A volume of 350μL of jelly was transferred to 12 of the 1cm x 1cm slots in a 1mL cube tray and allowed to cool for a further 10 minutes. Extracted DTG was weighed out at 1.00 ± 0.05mg and layered on the cooled jelly. The DTG layer was covered with 350μL cooled jelly. Twelve additional jelly blocks consisting of 700μL jelly without any DTG were prepared for controls. The jelly cube tray was covered to prevent any contamination and allowed to set at 4°C for 5 hours.

The dose prepared equates to the human dose of 50mg/day that is administered in both previously treatment-naïve and -experienced individuals.[31] The conversion of the human dose to a rodent dose was performed using the method reported by various researchers, that take size, surface area and metabolic rate into consideration.[136,137] At this dose, no toxicity was expected, as up to 15.95x time higher concentrations have been administered without resulting in toxicity.[138]

All rats were allowed a minimum of 1 week of acclimatization after weight matched division into experimental cage groups. During this period the animals were also trained to eat jelly blocks (containing no DTG) to habituate them to the manner in which DTG was administered

during the treatment period, to ensure optimal treatment administration. At 8 weeks of age, rats were entered into the treatment protocol in staggered fashion over one week to allow for sample collection logistics. At 8 weeks of age rats relate to approximately 4 years of age in humans and by 16 weeks it correlates to 10.5 years of age in humans.[139] During this time period the rodents are in a life stage that is equivalent to the adolescents to early adulthood developmental stage in humans.[140,141] The WHO considers individuals between 10 and 19 years of age to be within the adolescent developmental stage - making this a relevant age for this study, as DTG is prescribed at a dose of 50mg/day to PLWH older than 10 years of age and weighing more than 35. This is also the age following the initial growth spurt of the animals where the growth is expected to be more gradual, according to the Wistar rat growth curves published by Charles Fisher laboratories.[142] When the weight gain plateaus, it is easier to identify weight fluctuations amongst rodents.

The drug administration intervention lasted 12 weeks. All animals in the control groups received jelly blocks containing no treatment, while the DTG-treated group received jelly blocks containing DTG (preparation described in section 3.1). Because rats are nocturnal animals and DTG is prescribed to patients as a once daily dose often administered in the mornings to minimise the possibility of insomnia, a commonly reported side effect in patients, the animals were treated once daily at 14:00.

The jelly blocks were lifted out of the mould and one block given to each of the three rats in the cage simultaneously to prevent a rat from taking a jelly block from one another. Each cage was closely monitored during this time – to ensure that the entire block was consumed by the rat to which it was originally allocated to and allowing researchers to intervene should a jelly block be dropped or scavenged by other rats in the cage, thus ensuring each rat received the correct daily dose. The jelly blocks were generally consumed within 35 to 50 seconds whereafter the next cage was then administered their jelly blocks.

3.4 Sample collection

All animals were weighed bi-weekly and blood glucose concentration was measured as an end-point measure at the end of the 12-week intervention. At this time point, the rodents were euthanised using a lethal dose of sodium pentobarbitone (200mg/kg), injected

intraperitoneally by a registered veterinarian. Approximately 8mL blood was drawn from the heart by the registered veterinarian and collected in equal volumes in ethylenediaminetetraacetic acid (EDTA) and Heparin tubes. The tubes were gently inverted multiple times to ensure homogenous distribution of the respective anticoagulants. Death was confirmed by exsanguination and cessation of circulation by transecting the aorta.

The right retroperitoneal AT depot was dissected from the abdominal cavity of the rat. A portion of the AT was snap frozen and stored at -80°C for subsequent batch analysis using commercial ELISA and colorimetric assays. The remainder of the AT was embedded in tissue freezing medium (OCT; 14020108926, Leica Biosystems Nussloch GmbH, Germany), snap-frozen in liquid nitrogen and stored at -80°C until sectioning for histological analysis.

In order to fully utilise the carcasses, other organs which include the liver, brain, gut, aorta, gastrocnemius muscle, were harvested for DTG-related analyses by other postgraduate students in our research group. All organs and AT depots were weighed on a precision electronic balance (XY10002C, readability: 0.01g, maximum weight: 1100g, Axiology) before processing.

3.5 Adipokine and cytokine analysis

Plasma and AT cytokine profiles were assessed using commercially available ELISA kits to determine concentrations of IL-10 (E-EL-R0016, Elabscience, sensitivity: 18.75pg/mL, range: 31.2 –2000pg/mL), TNFα (E-EL-R2856, Elabscience, sensitivity: 9.38pg/mL, Range: 15.63-1000pg/mL), MCP-1 (E-EL-R0633, Elabscience, sensitivity: 0.1ng/mL range: 0.16-10ng/mL), IL-1β (E-EL-R0012, Elabscience, sensitivity: 18.75pg/mL range: 31.25- 2000pg/mL), Resistin (E-EL-R0614, Elabscience, sensitivity: 0.19ng/mL range: 0.31-20ng/mL), and adiponectin (E-EL-R3012, Elabscience,sensitivity: 0.94ng/mL range: 1.56-100ng/mL). The %CV for all kits was < 10%. In addition, a commercially available myeloperoxidase (MPO) colorimetric activity assay kit (E-BC-K074, Elabscience) was employed to determine MPO level, as indicator of pro-inflammatory cell activation. For both the ELISA and MPO colorometric assay, AT samples were homogenised using a bead mill homogeniser (BEAD RUPTOR ELITE, OMNI international). Frozen AT was weighed and added to ice cold phosphate buffered solution (PBS) in a 550mg:1000uL ratio. The tissue samples were homogenised at a speed of 4m/s

for 3 cycles of 20 seconds with 1-minute intervals, where the samples were placed on ice between each cycle. The samples were then centrifuged for 12 minutes at 10,000 x *g* at 4°C before supernatants were collected, aliquoted and stored at -80°C until analysis. All samples were thawed on ice prior to analysis and kept on ice for the duration of the process. The cytokine levels were assessed following the protocol provided by the ELISA and MPO assay kit manufacturer and the absorbances read using a VictorNivo absorbance plate reader at a wavelength of 450nm for ELISA kits and 460nm for the MPO assay. Sample supernatant protein content was determined using the Bradford method.[143] Results obtained from the ELISA kit assays were expressed as picograms/ microgram (pg/µg) protein.

3.6 Adipose tissue histology

Collected AT was initially embedded in OCT, with the intention of characterization of macrophage subpopulatons in the tissue, using immunofluorescence staining, brightfield microscopy and semi-automated image analysis. However, rodent AT proved exceptionally difficult to section. Even a laboratory technician with years of experience cutting human adipose biopsies processed exactly the same way, was unable to produce good quality sections. Therefore, the decision was made to rather probe the ability of DTG to polarize macrophages in an *in vitro* pilot study (described below in section 3.8) and to focus on the general AT profile (fibrosis, adipocyte size) of the rodent AT. In order to facilitate sectioning of the AT, AT samples were removed from the OCT and thawed in 4% buffered paraformaldehyde, allowing for a minimum of 1 day to fix the tissue, after which the tissue was processed using a tissue processor (Leica HistoCore Pearl, Leica Biosystems Nussloch GmbH, Germany), impregnated in a tissue processor (Leica HistocCore Pearl, Leica Biosystems Nussloch GmbH, Germany) and embedded in paraffin wax (Leica HistoCore Arcadia H, Leica Biosystems Nussloch GmbH, Germany) whereafter it was sectioned at 5 µm on a rotary microtome (Leica RM2125 RTS). AT sections were deparaffinized in xylene and rehydrated in decreasing ethanol concentrations before being stained using haemoloxylin and eosin (H&E), and Masson's Trichrome stain (Leica Autostainer XL, Leica Biosystems Nussloch GmbH, Germany). Finally, slides were mounted with mountant (DPX, 06522, Sigma- Adrich, USA) and fitted with coverslips for viewing.

3.7 Image acquisition

All histological slides were viewed using an inverted microscope (Nikon eclipse Ti2, Japan) mounted with a camera (LWD 0.52 Nikon, Japan). Image processing was done on Nikon Instrument Software (NIS- Elements D 5.30.02 64-bit) on a desktop computer (Dell, USA) running Windows 7 (Microsoft, USA). Three representative images of each section were captured at 10x magnification with an additional 10x magnification on eye the piece (i.e.x100 magnification).

3.7.1 Image analysis H&E

Once images were acquired, they were analyzed using Image J software (version 1.49). The 100μm scale bar was measured using the straight-line tool and the measurement was imported to the "set-scale function" allowing cell area to be recorded in μm^2. The border of 50 adipocytes representative of the cell population were traced using the polygon selection tool to measure and record cell area on each of the three representative images.

At this time it became evident that the abundance of macrophages in AT was to low to allow for accurate assessment of phenotypes. Therefore, the decision was made to rather investigate this aspect *in vitro.* (refer to section 3.8).

3.7.2 Image analysis of Masson's trichrome

Once the images were acquired, they were analysed using Image J software (version 1.49, Wayne Rasband) with the Colour Deconvolution plug-in as developed by Landini (version 1.5). The image was then processed using Colour Deconvolution; the plug-in provides a number of built-in stain vectors. The images acquired from the sections stained with Masson's trichrome were processed using the Masson's trichrome option. Briefly, the plug-in unmixes a RGB image into three 8-bit images with a colour look up table that corresponds to the respective vector colours. The analysis measurements were set to measure 'area', 'area fraction', 'limit to threshold', and 'display label'. The threshold of each of the three images was

adjusted allowing measurement of 1) the background and 2) connective tissue. Percentage fibrosis was calculated as follows: % area background fibrosis subtracted from % area connective tissue fibrosis.

3.8 *In vitro* assessment of DTG-associated macrophage polarization

As mentioned above, the aim of this experiment was to assess potential effects of DTG on macrophages phenotype expression.

Due to limited reagents at our disposal, experiments could not be repeated enough times to ensure repeatability of outcome, so this study should be considered a pilot study only.

3.8.1 Ethical clearance and blood collection

Ethics exemption for the use of donor blood in *in vitro* assays were obtained from Stellenbosch University Subcommittee C Health research ethics committee (SU Subcom C HREC) (reference: X15/05/013, refer to appendix 2). Peripheral blood samples were collected in 10mL EDTA vacutainer plastic blood collection tubes and gently inverted multiple times to thoroughly mix the ETDA anti-coagulant and the blood. Samples were maintained at room temperature and processed within 30 minutes after collection.

3.8.2 Monocyte isolations by double gradient centrifugation

Whole blood monocytes were isolated from whole blood samples by means of two consecutive density gradient centrifugation steps. This experiment was performed at room temperature. Initially, 8 mL whole blood was carefully layered onto 4mL histopaque 1.077 (10771-100ML, Sigma) and centrifuged at 400 x *g* for 30 minutes. The opaque layer at the interface of the blood plasma and histopaque 1.077 was then collected with a Pasteur pipette and transferred to a 15mL falcon tube containing 1mL of 1mM PBS-EDTA solution – this prevents clumping of the cells. After the opaque layer was transferred to the tube, additional 1mM PBS-EDTA solution was added to each tube to reach a final volume of 7mL. The samples were then centrifuged at 300 x *g* for 10 minutes. The supernatant was aspirated, and the resulting cell pellets were resuspended in culture media (RPMI-1640 without phenol red

(R7509, Sigma-Aldrich) supplemented with 10% (v/v) foetal bovine serum (FBS; 10493-106, Gibco) and 1% (v/v) Penicillin/Streptomycin (PenStrep; DE17-602E, BioWittaker, Lonza). This cell suspension was layered on a 46% iso-osmotic Percoll solution and centrifuged at 550 x g for 30 minutes.

46% iso-osmotic Percoll solution was prepared by mixing 6.939 mL Percoll solution (density: 1.131g/mL) (E0414, Sigma-Aldrich) with 0.561 mL 10x PBS – of this a volume of 6.9mL was transferred to a new microcentrifuge tube to which 8.1mL RPMI-1640 with phenol red (R8758, Sigma- Aldrich) supplemented with 10% (v/v) FBS was added.

The white ring of cells between the two phases was collected and added to 15mL microcentrifuge tube containing 1mM PBS-EDTA and centrifuged at 400 x g for 10 minutes. The resulting cell pellet was resuspended in 1mM PBS-EDTA and the centrifugation step repeated. After the second centrifugation step, the supernatant was aspirated and the cell pellet resuspend in RMPI-1640 supplemented with 10% (v/v) FBS and 1% (v/v) PenStrep and plated according to experiment specifications.

3.8.3 Monocyte differentiation and macrophage polarization

Isolated monocytes were plated at a density of 1x10^6 cells per well in 24-well culture plates and cultured in what will from here on be referred to as complete monocyte media. This consisted of RMPI-1640 supplemented with 10% (v/v) foetal bovine serum and 1% (v/v) penicillin/streptomycin. The cells were maintained in monocyte complete media supplemented with either 50ng/mL GM-CSF or 50ng/mL M-CSF at 37°C, 5% CO_2 in a humidified incubator. The protocol used to differentiate and polarise the cell to the respective phenotypes included a 7-day differentiation period and a 24-hour polarisation period.

To polarize the cells to the M1 phenotype, the cells were pre-treated by supplementing monocyte complete media with 50ng/mL granulocyte macrophage colony-stimulating factor (GM-CSF; SPR3050, Sigma-Aldrich). Initially, the cells were allowed to adhere to the culture platecot for 24 hours prior to the first media change. The cells were refreshed every 72 hours with fresh media that contained 50ng/mL GM-CSF. After 7 days the GM-CSF pre-treated cells were supplemented with 50ng/mL GM-CSF, 50 ng/mL lipopolysaccharide (LPS; L7262,

Sigma-Aldrich) and 20ng/mL interferon-γ (IFN-γ; I3265, Sigma- Aldrich) and allowed to incubate for 24 hours.

To polarise the cell to the M2 phenotype, a similar protocol was followed except the reagents used as pre-treatment and differentiation stimuli differed. The cells were pre-treated with 50ng/mL monocyte colony-stimulating factor (M- CSF; SRP3110, Sigma Aldrich) for 7 days. M-CSF pre-treated cells were exposed to 20ng/mL IL-10 (SRP3071, Sigma Aldrich), 20ng/mL IL-4(SRP4137, Sigma-Aldrich) and 20ng/mL transforming growth factor- β1(TGF-β; T7035, Sigma-Aldrich) for 24 hours.

Both sets of polarised cells were treated with DTG with dimethyl sulfoxide (DMSO; D2650, Sigma-Aldrich) as a vehicle. The concentration highest concentration of DMSO were 0.1%. Two vehicle controls (one for the M1 and one for M2 phenotype) exposed to the highest concentration of DMSO were run in parallel.
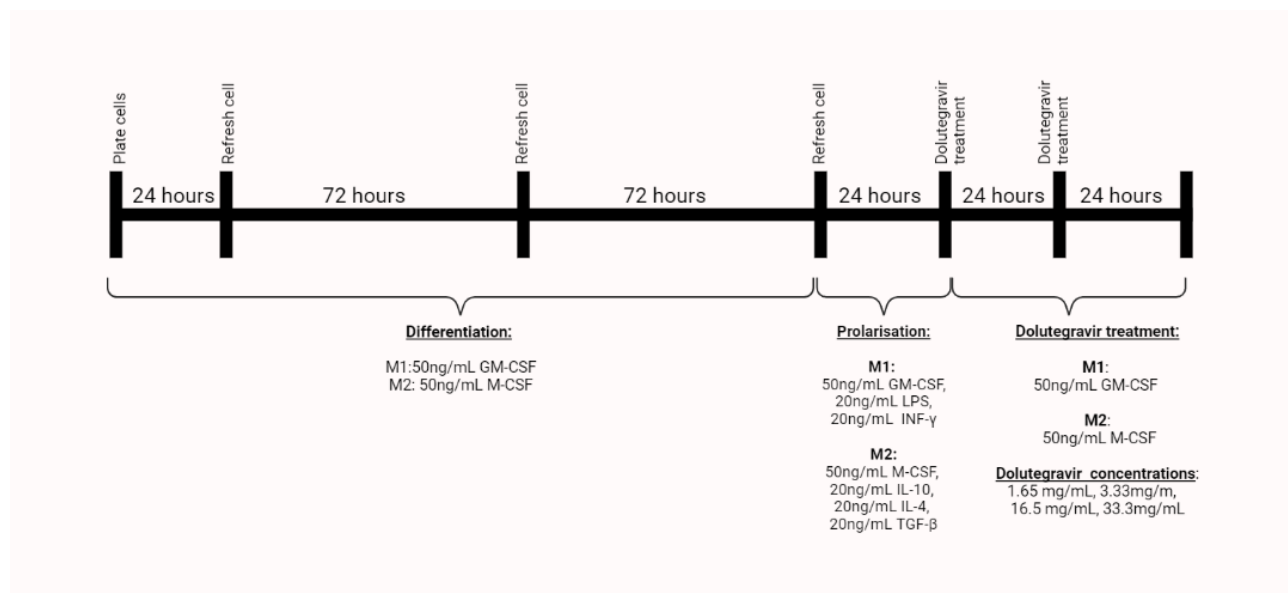

Figure 3.1: Differentiation, polarization and dolutegravir treatment. *Visual presentation of the timeline for the monocyte differentiation, polarization, and treatment protocol with the relevant monocyte complete media supplementations requirements for inducing and treating M1 and M2 macrophage phenotypes.*

3.8.4 Dolutegravir treatment

As there is no concrete information available regarding the bioavailability of DTG at AT level, cells were treated with a dose converted from the human administered dose (3.33mg/mL),

35

although higher and lower concentrations were included in the experiment. The various concentrations were included to mimic decreased bioavailability (1.65mg/mL) and drug accumulation (16.5mg/mL and 33mg/mL). These doses were included as a result of the controversy regarding DTG distribution in AT. One study suggests poor distribution into adipose[9] whereas another suggest the contrary[5] with potential accumulation not yet fully elucidated.

Because of the poor solubility of DTG in water, a 1mg/mL stock solution was prepared by dissolving extracted DTG in DMSO. This was prepared fresh each day to avoid freeze-thaw of the stock solution. The stock solution was used to supplement the monocyte complete media to reach appropriate concentrations. The final DMSO concentration was less than 0.5% and a vehicle control was included to account for the potential effects that the DMSO might impose on the phenotypic shift. The cells were treated for a total of 48 hours with media being replaced every 24 hours as the half-life of DTG is only 12-15 hours. Although it would have been ideal to have 12-hourly treatment intervals, previous experiments showed significant cell loss as a result of excessive handling.

3.8.5 Phenotype determination by flow cytometry

Accutase® solution (A6964, Sigma-Aldrich) was used to detach the cells from the culture plate. The cells that remained adhered were gently scraped from the plate surface using a cell scraper. The cells were collected and counted using a haemocytometer whereafter the cells underwent centrifugation (400 x g for 5 minutes) and were resuspended in the appropriate volume of staining buffer (PBS containing 20% FBS, filtered) to reach a final cell concentration of $1x10^6$ cells/mL. 200μL of the control sample were then transferred to a 5mL FACS tube- this sample was used as the unstained control. Cells in the 5mL FACS tube were resuspended in 1mL staining buffer, centrifuged (400 x g for 5 minutes), the supernatant discarded, and the pellet resuspended in 1mL staining buffer without any added antibodies.

The remaining cells were washed in 1mL staining buffer centrifuged (400 x g for 5 minutes), resuspended in 1mL staining buffer, 50μL (1:100) Human BD Fc block (564219, BD Pharmingen, BD Bioscience) and incubated for 20 minutes in the dark at 4°C whereafter the cells were centrifuged for 10 minutes at 250 x g, the supernatant aspirated and discarded.

36

The cells were resuspended in 50μL permeabilization/wash buffer (51-2091KZ, BD Bioscience) containing surface marker antibodies CD-68 -BV421 (562643, BD Bioscience), CD206-BB515 (564668, BD Bioscience) and viability780 (565388, BD Bioscience). Cells were then incubated for 30 minutes in the dark at 4 °C. The cells were washed by resuspension in 1mL staining buffer followed by 10-minute centrifugation at 250 x *g*.

After centrifugation the supernatant was discarded, and the cells resuspended in 250uL fixation and permeabilization solution (51-2090KZ, BD Bioscience) and incubated in the dark for 15 minutes (4 °C). The wash step was repeated, and the cell pellet resuspended in 1mL staining buffer containing intracellular antibodies IL-10-PE (559330, BD Bioscience). This was followed by a 30-minute incubation step in the dark (4 °C). The cells were then washed with staining buffer and were resuspended in 300μL staining buffer before data acquisition.

3.8.6 Flow cytometry

Cell phenotype and the associated fluorescent signals were analysed using a Cytek ® Aurora with autoloader (Cytek bioscience, Inc. Fermont, CA) instrument with SpectroFlow version 2.2.0.4 software (09032020). A total of 10 000 events were recorded for each sample prior to analysis using FlowJo_v10.8.1x (BD bioscience) software. Gating parameters were previously determined using fluorescence minus one (FMO) and single stain controls.

3.9 Statistical analysis

Statistical analysis was performed using GraphPad Prism v.8 software. All outliers were identified and excluded from the data sets. Data is presented as mean ± standard deviation (SD). All data were assessed for normality using Shapiro-Wilks analysis. Parametric data was analyzed using two-way ANOVA to determine differences between the male and female groups with and without DTG treatment. Tukey's multiple comparisons were implemented as post-hoc test. Alternatively, non-parametric data were analyzed using Kruskal-Wallis tests with Dunn's multiple comparisons. Correlations were evaluated by calculating Pearson's correlation coefficient. The level of statistical significance was set at $P<0.05$.

Chapter 4: Results

4.1 Body and organ mass

On average the treated and control animal groups gained weight at a similar rate over the course of the study (Fig. 4.1). At the protocol endpoint, male rodents exhibited significantly higher body mass compared to females as expected (Fig. 4.2), but no significant effect of DTG treatment was observed.
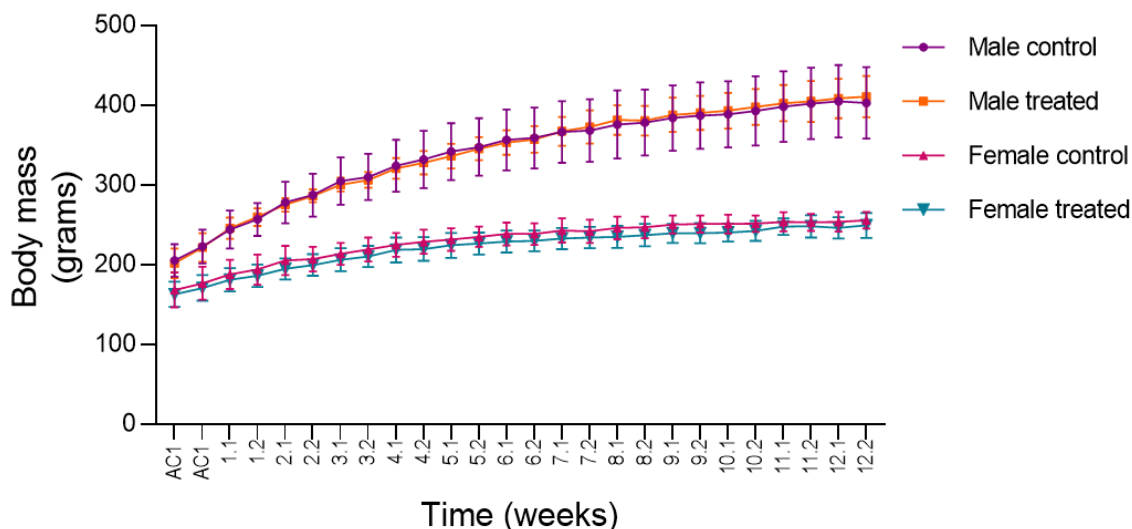

Figure 4.1: Body mass. *The change body mass of the animals as recorded over the course of the acclimation and 12- study period. Data is presented as mean body mass for each experimental group (n=6) at biweekly intervals with error bars indicating standard deviation (SD). (AC; acclimation)*
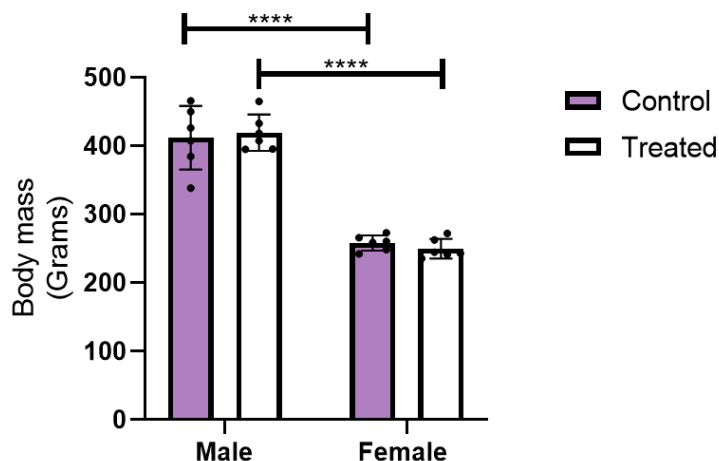

Figure 4.2: Endpoint body mass. *Average endpoint body mass (in grams) of receptive experimental groups expressed as mean body mass ± SD. Statistical analysis: Two-way ANOVA with Tukey's multiple comparison post-hoc test. **** p<0.0001*

No significant differences between controls and DTG-treated groups were observed in terms of organ masses assessed (Table 4.1). Although not directly relevant to the thesis topic, an interesting observation was that females in general had a larger brain mass relative to body mass compared to males, while other organs showed no sex difference (Fig 4.3).

Table 4.1: organ mass. This table depicts the average mass of the brain, the total (left- and right-) retroperitoneal AT depots, the liver, and the gastrocnemius muscle at protocol endpoint in grams. The values are expressed as the mean mass ± SD, n=6

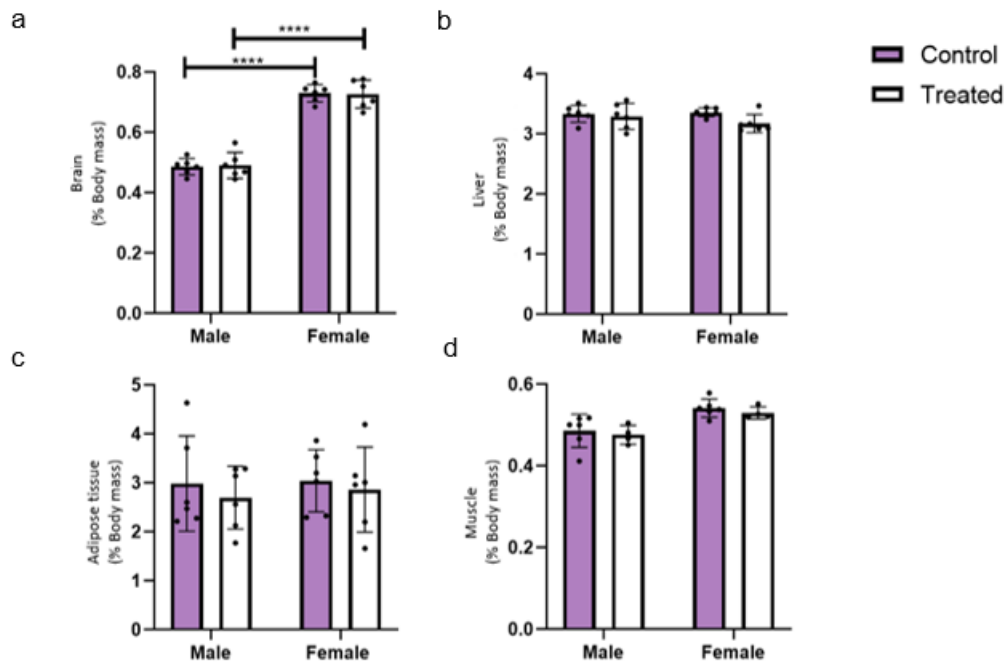|	Brain	Retroperitoneal adipose tissue depots	Liver	Gastrocnemius muscle
Control Females	1.88 ± 0.09	7.87 ± 1.72	8.67 ± 0.38	1.41 ± 0.90
Treated females	1.81 ± 0.08	7.19 ± 2.27	7.49 ± 0.80	1.32 ± 0.60
Control male	2.00 ± 0.13	12.60 ± 5.28	13.76 ± 1.77	1.89 ± 0.22
Treated males	2.05 ± 0.11	11.32 ± 2.95	13.84 ± 1.67	2.04 ± 0.13

*Figure 4.2: Organ mass. a- Mass of dissected rat brains b- liver weight c- retroperitoneal AT depot weight d- gastrocnemius muscle weight. Expressed as mean percentage of the body mass (tissue mass / body mass x100) ± SD (n=6). Statistical analysis: Two-way ANOVA. **** p<0.0001.*

39

4.2 Blood parameters

Blood glucose concentrations were within the expected normal range (3.95 ±1.31mmol/L)[144] for all animals and did not differ between treatment or sex groups (Fig 4.4).
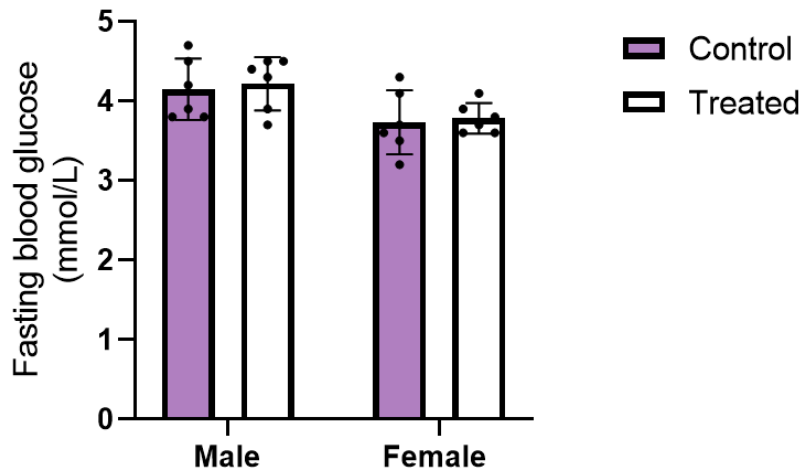

Figure 4.4: Fasting blood glucose. *Average fasting blood glucose (mmol/L) levels of respective experimental groups as an endpoint measure. Statistical analysis: Two-way ANOVA with Tukey's multiple comparison post-hoc test.*

Circulating levels of the various cytokines were measured to correlate circulating cytokines levels with tissue cytokine levels. However, plasma concentrations were below the assay kit detection threshold for adiponectin, resistin, TNF-a, IL-1β and IL-10. This data was thus excluded from further analysis and interpretation.

4.3 Adipose tissue signaling profile

The levels of IL-10 and IL-1β in AT were below the lower limit of quantification of the assay kit. Average levels of MCP-1 in the AT homogenate were slightly higher in females than males (Fig 4.5 b), but no statistically significant sex or treatment effect was evident. Neither resistin, nor adiponectin seemed to be affected by DTG, with no significant sex differences evident (Fig. 4.6 a,b).
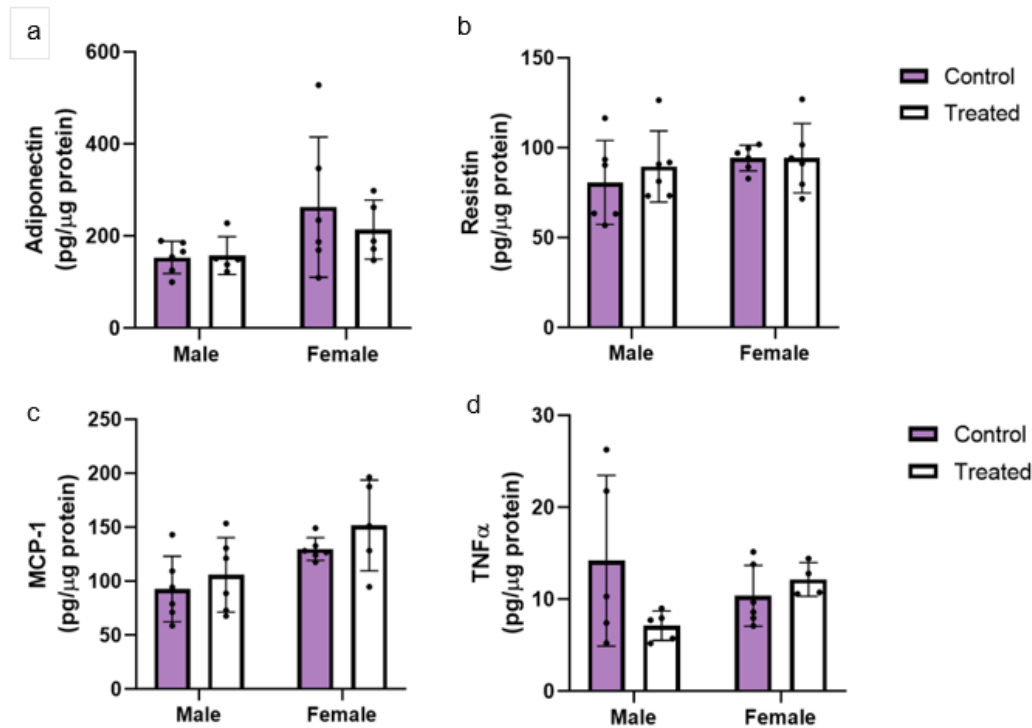
Figure   *3.5:*
Pro-inflammatory cytokines. *a- VAT adiponectin levels (pg/µg protein b- VAT resistin levels (pg/µg protein). c- MCP-1 levels in adipose as detected in AT homogenate (pg/µg protein). d- TNF-α levels in AT homogente (pg/µgprotein) Graphs depicted shows the group means ± SD. Statistical analysis: Two-way ANOVA.*

Adjusting results for bodyweight and AT mass (Fig. 4.6 a-g) did not change the outcome in terms of DTG but did illustrate higher relative levels of all parameters in females vs males, although not all reached statistical significance.
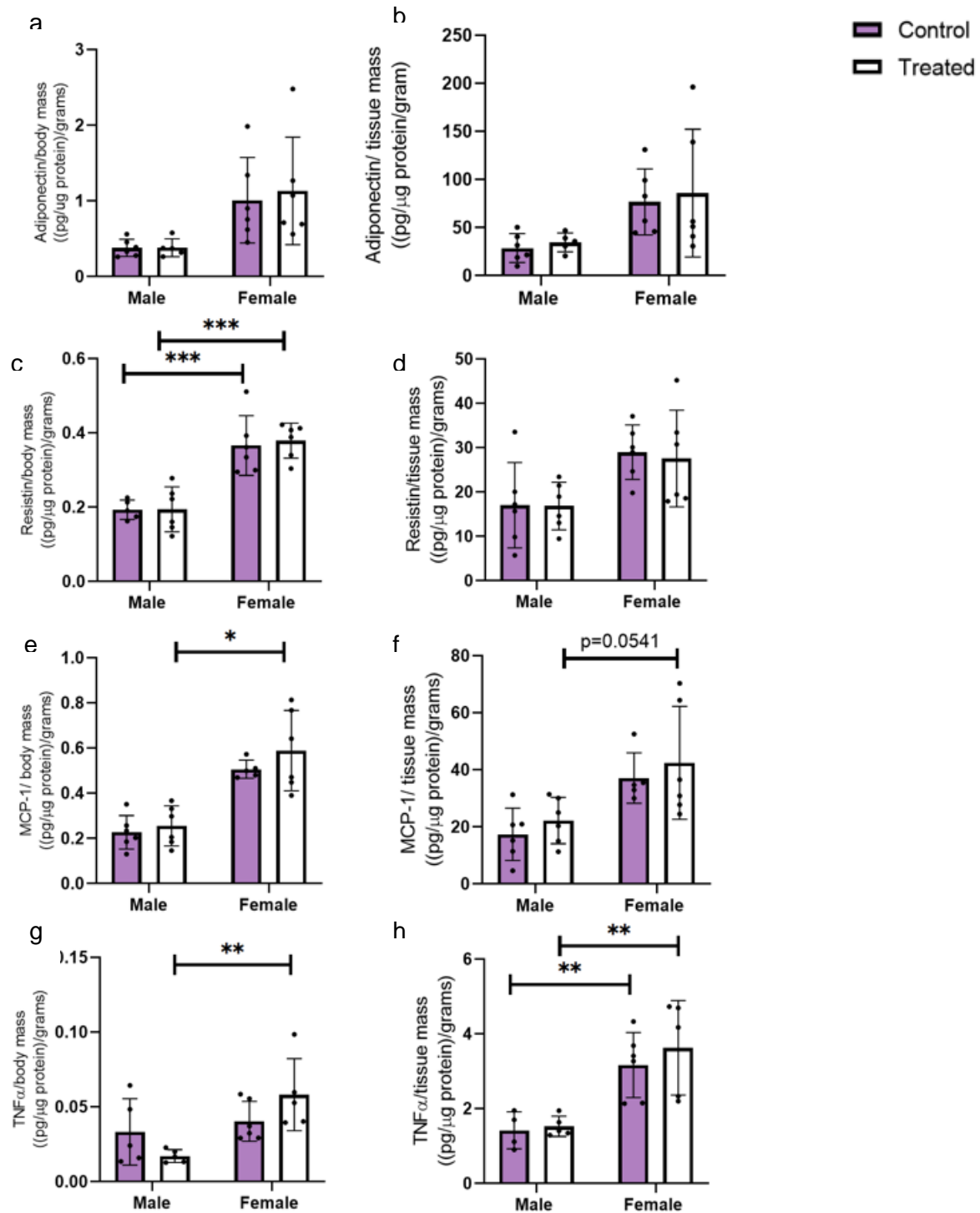
Figure 4.6 cytokines corrected for body mass and adipose tissue mass: *a – mean adiponectin levels (pg/μg protein) per gram body mass. b- mean adiponectin levels (pg/μg protein) per gram tissue c- mean resistin levels (pg/μg protein) per gram body mass d- mean resisitn levels (pg/μg protein) per gram tissues e- mean MCP-1 levels (pg/μg protein) per gram body mass f- mean MCP-1 levels (pg/μg protein) per gram tissue mass g- mean TNF-α levels (pg/μg protein) per gram body mass h- mean TNF-α levels (pg/μg protein) per gram tissue mass. Data is expressed as groups means ± SD; n=6.*

42

4.4 Adipose tissue histology

Representative images illustrating AT general morphology are presented in (Fig 4.7) In general, the adipocytes in male retroperitoneal AT showed trends of being larger than the adipocytes measured in the female retroperitoneal AT depot. Although not significant the adipocytes in the rats treated with DTG appeared to be smaller than those in the control groups, especially in the females.
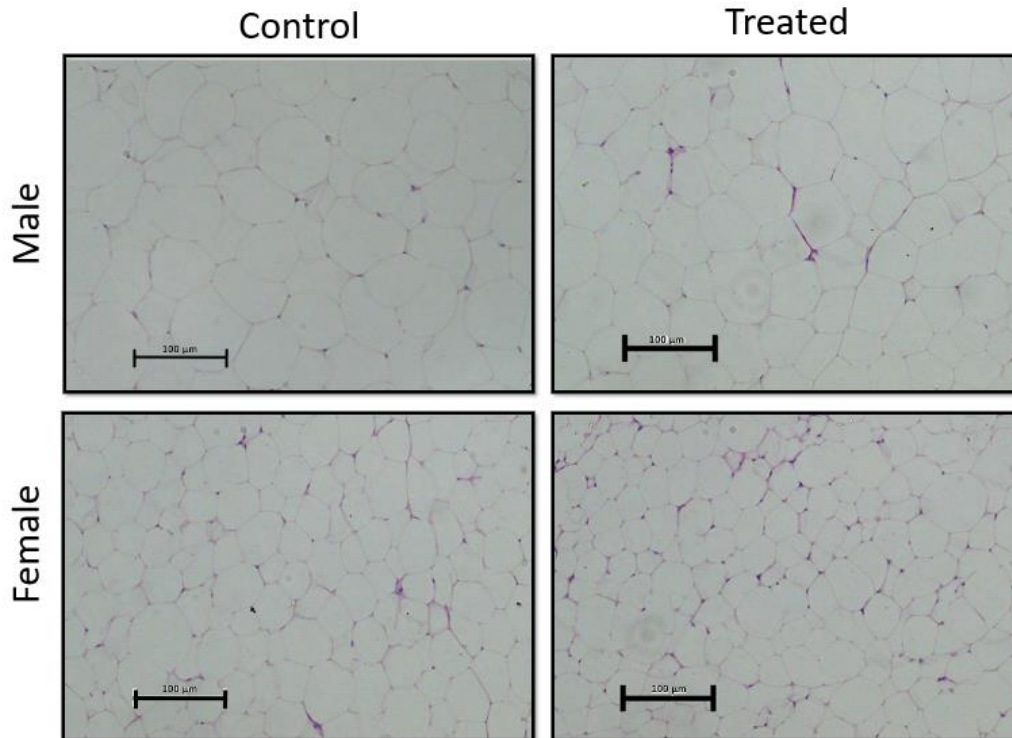

Figure 4.7 Adipocyte morphology. *Representative images of histological sections stained with H&E.*
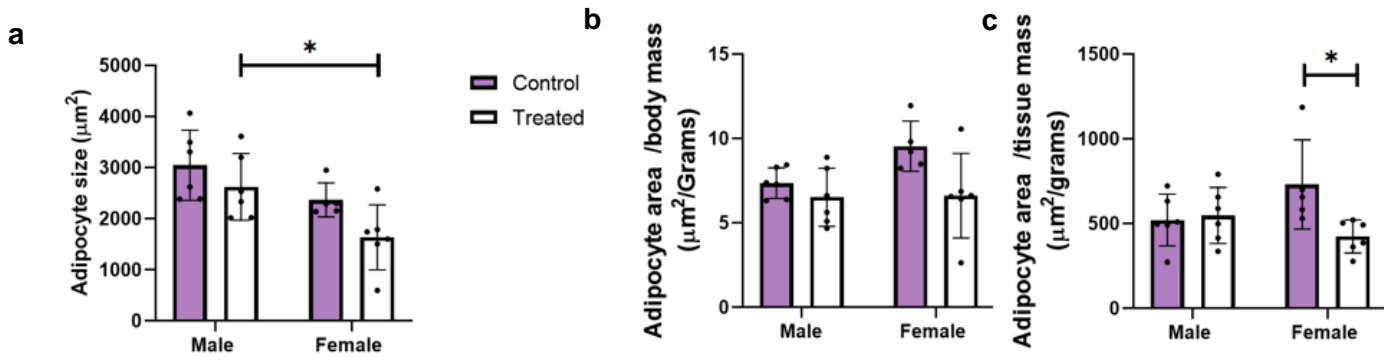
Figure 4.8: Average adipocyte size. *a- The average surface area (μm²) of 50 adipocytes measured on 3 representative images for each animal b- The average adipocyte surface area per gram body mass (μm²/ gram). C- the average adipocyte size per gram AT mass. Data is expressed as mean ± SD. Statistical analysis: two-way ANOVA *p<0.05. (n=6).*

AT across all groups showed very limited signs of fibrosis (Fig 4.9), with no effect of sex or DTG treatment (Fig. 4.10)
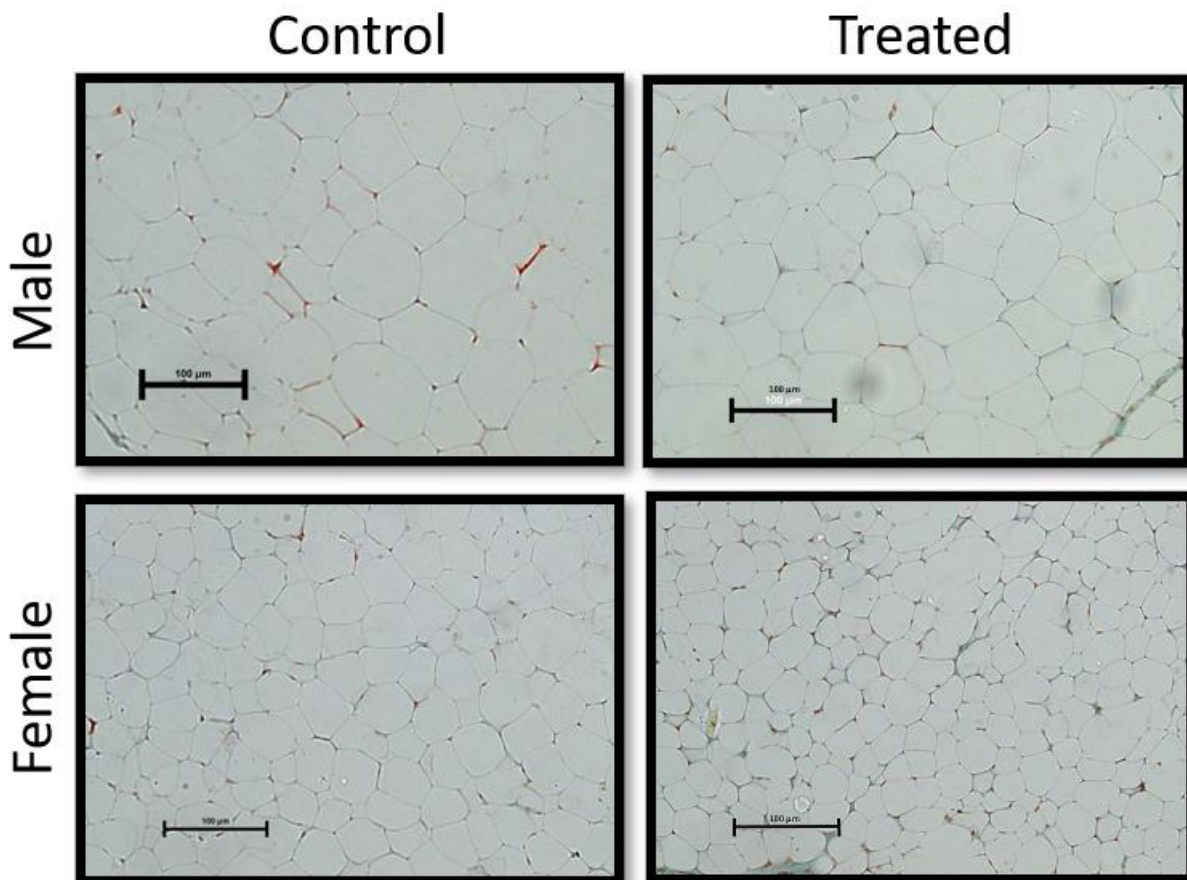

44

Figure 4.9: Adipose tissue fibrosis. *Representative images stained with Masson's trichrome to assess fibrotic profile of AT.*
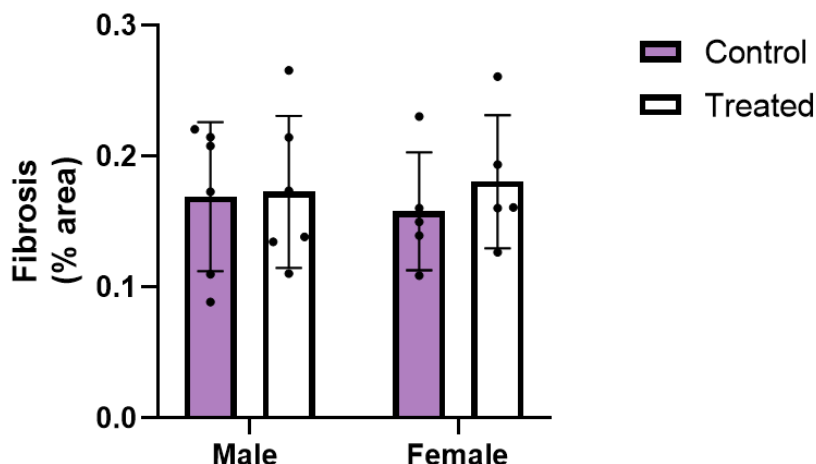

Figure 4.10: Adipose tissue fibrosis. *Mean AT fibrosis expressed as % surface area. Statistical analysis: Two-way ANOVA.*

4.5 Macrophage phenotyping.

The data represented below was obtained after treating differentiated and polarized M1 and M2 macrophages with various concentrations of DTG. This was done in order to assess the potential of DTG to induce a phenotypic shift in macrophages and to predict if it in turn contributes to a more pro – or anti- inflammatory microenvironment. Because we had limited reagents at our disposal, the experiment was conducted only once to probe these effects.

Preliminary data illustrates that in macrophage pre-polarised to a M1 phenotype, CD68 expression tended to be lower at low concentrations (1.65 and 3.33µg/mL) of DTG, while the expression in the M2-polarised phenotype was higher at high concentrations (16.6 and 33.3µg/mL) (Fig. 4.11 and 4.12). CD 68 is regarded an M1 marker – suggesting that at lower concentrations DTG might induce anti-inflammatory effects in the M1 polarised macrophages. High concentrations are then thought to induce pro-inflammatory effects by increasing the CD68 markers in the M2 polarised macrophages.

While IL-10 expression in the M1-polarised population was increased at lower DTG concentrations (1.65 and 3.33µg/mL), expression of IL-10 decreased with increased concentrations of DTG in the M2-polarised populations (Fig 4.17 and 4.18). Together, these parameters consistently suggest that low doses of DTG seemed to exert a phenotype switch to a relatively more anti-inflammatory phenotype, while higher doses had the opposite effect.

Due to the configuration and setup of the instument issues it is not possible to draw any concrete conclusions on the data abtained from quantifying CD206.
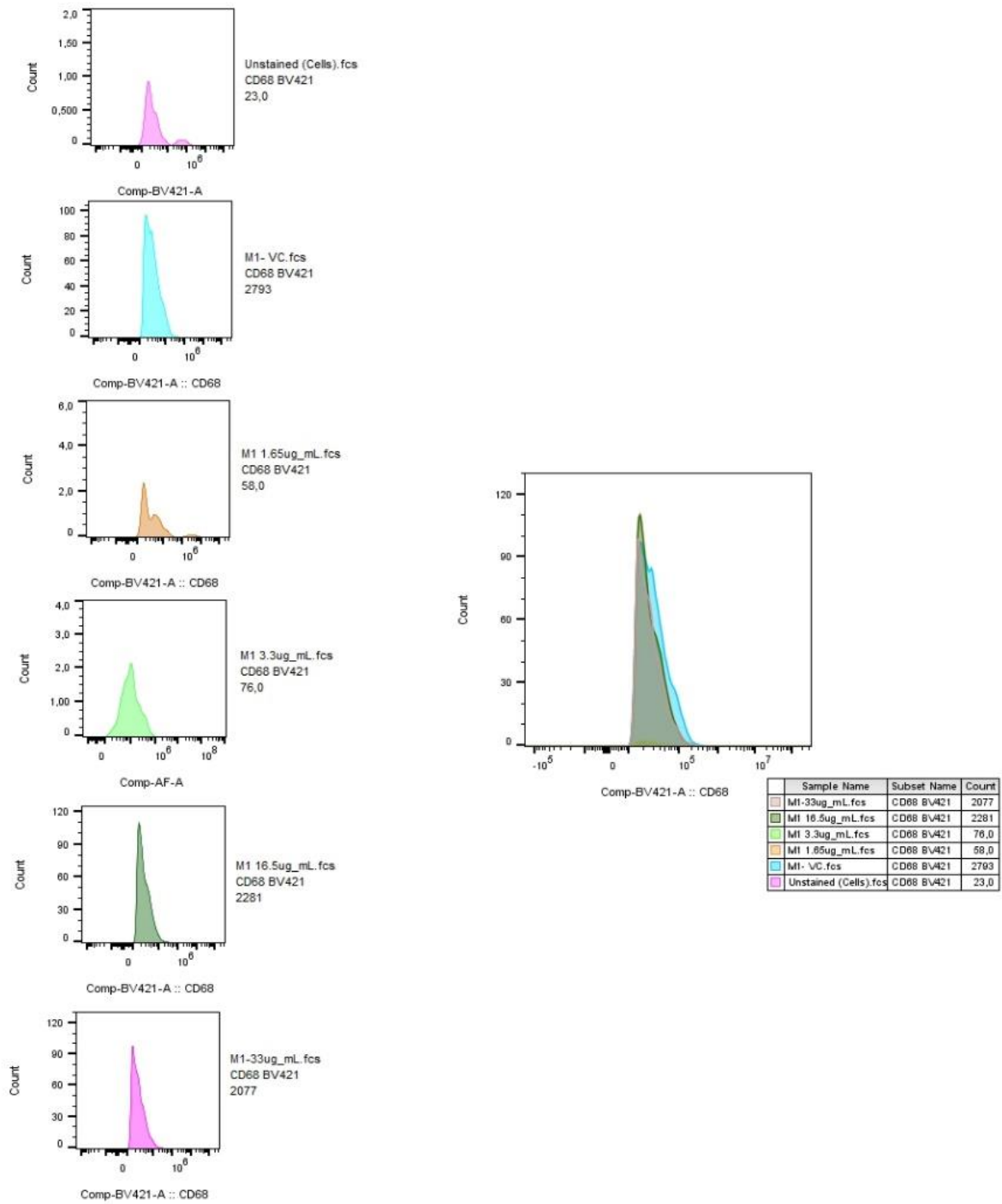
Figure 4.11: CD 68 marker M1 macrophages. *This figure represents the flow cytometer data and illustrates the expression of CD68 on M1 polarized cells treated with various concentrations of DTG and in a combined graph.*
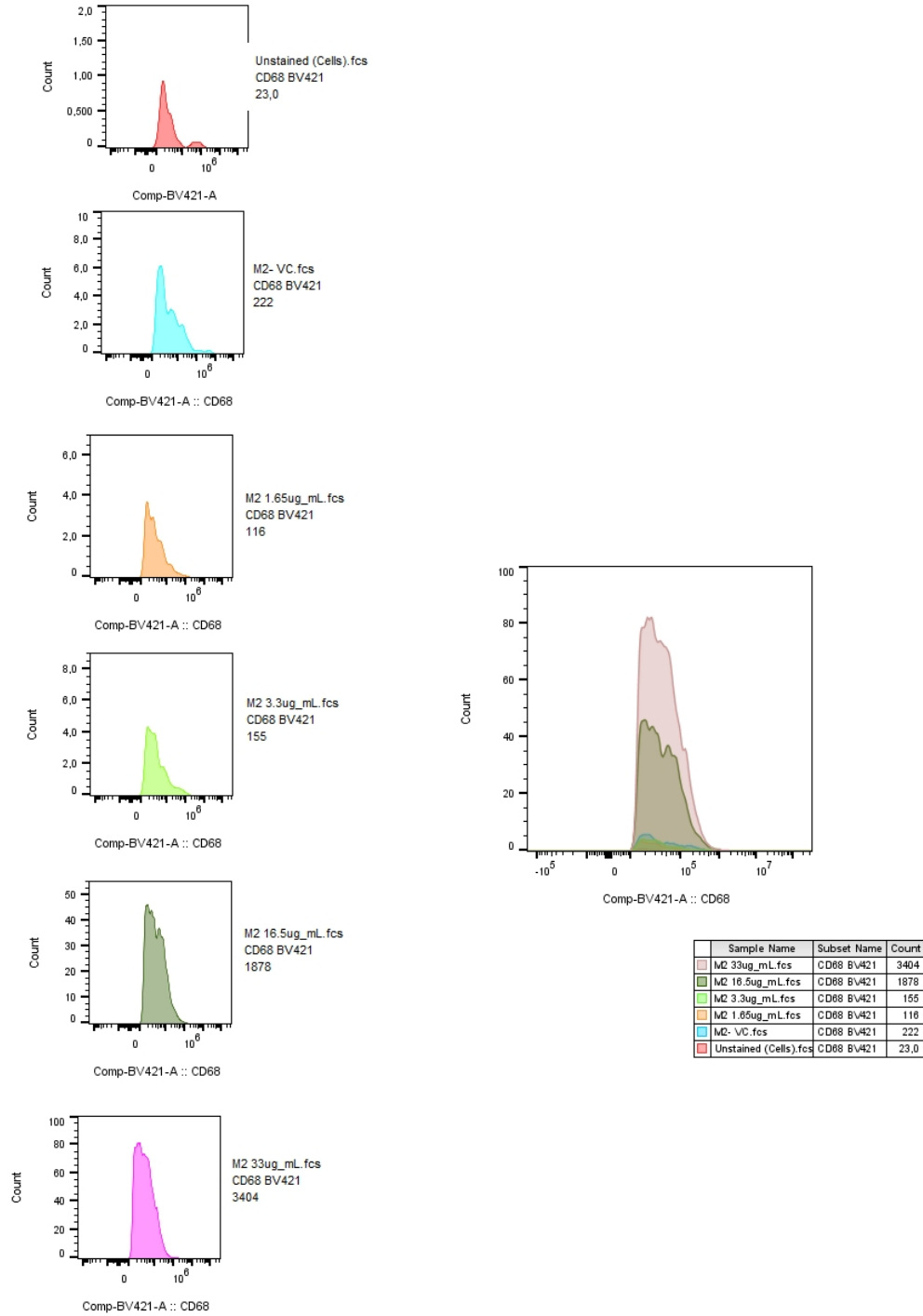
Figure 4.12: CD 68 marker M2 macrophages. *This figure is a representation of DTG treated M2 polarised cells' expression of CD68.*
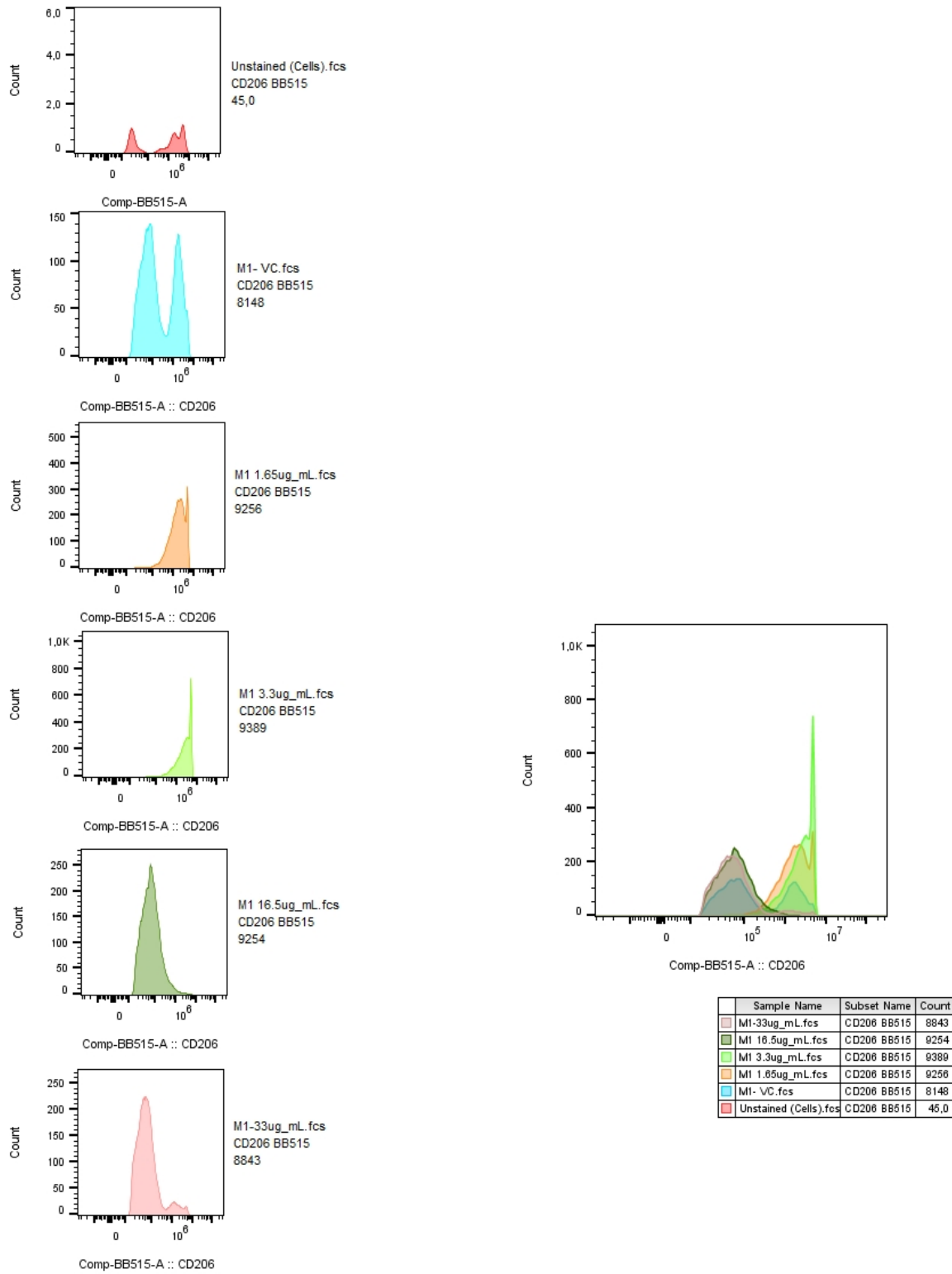
Figure 4.13: CD 206 marker M1 macrophages. *This figure illustrates the expression of CD206 on M1 polarized cells treated with various concentrations of DTG.*
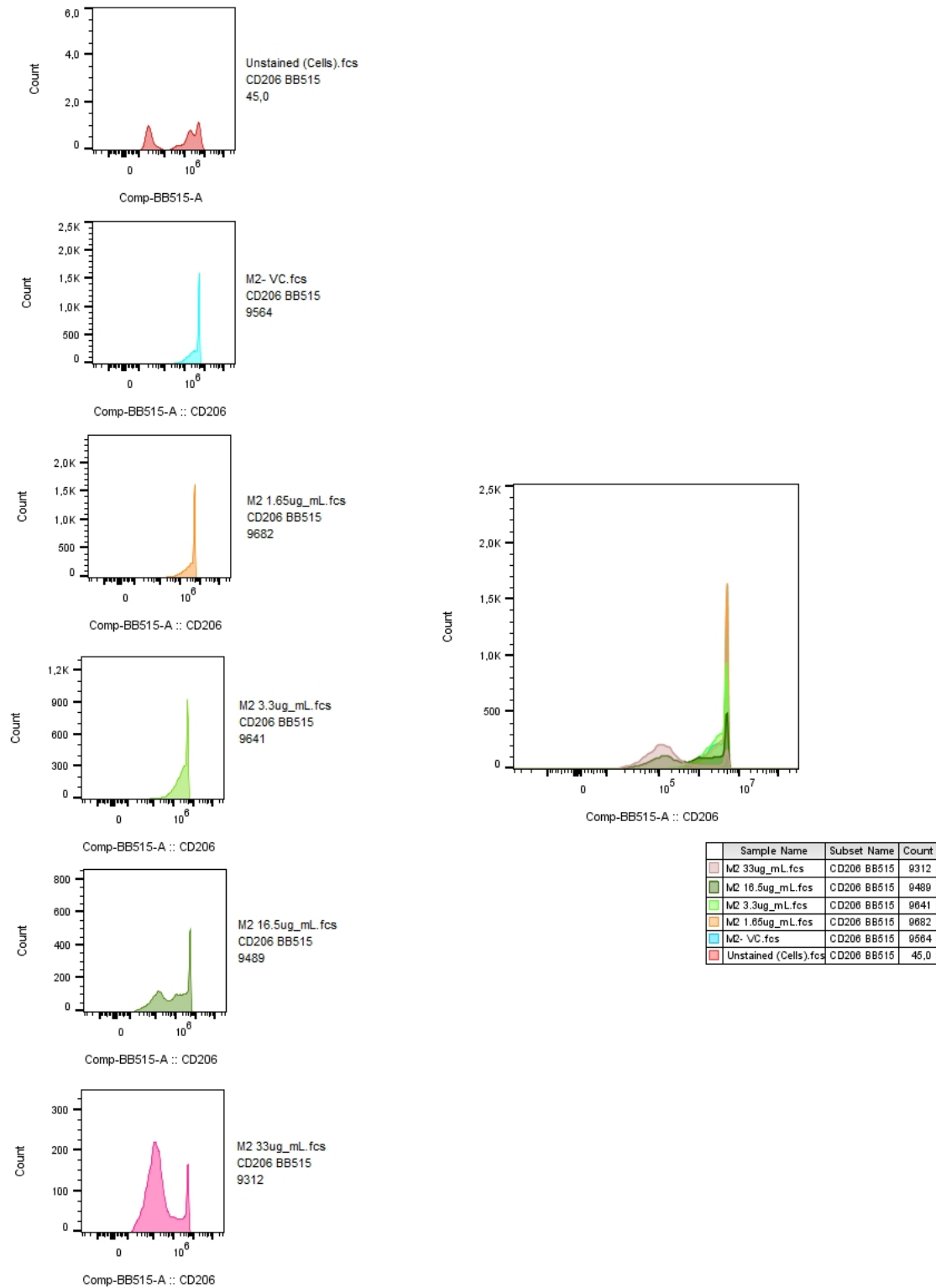
Figure 4.14: CD 206 marker M2 macrophages. *DTG effects on CD206 expression in M2 polarised cells.*
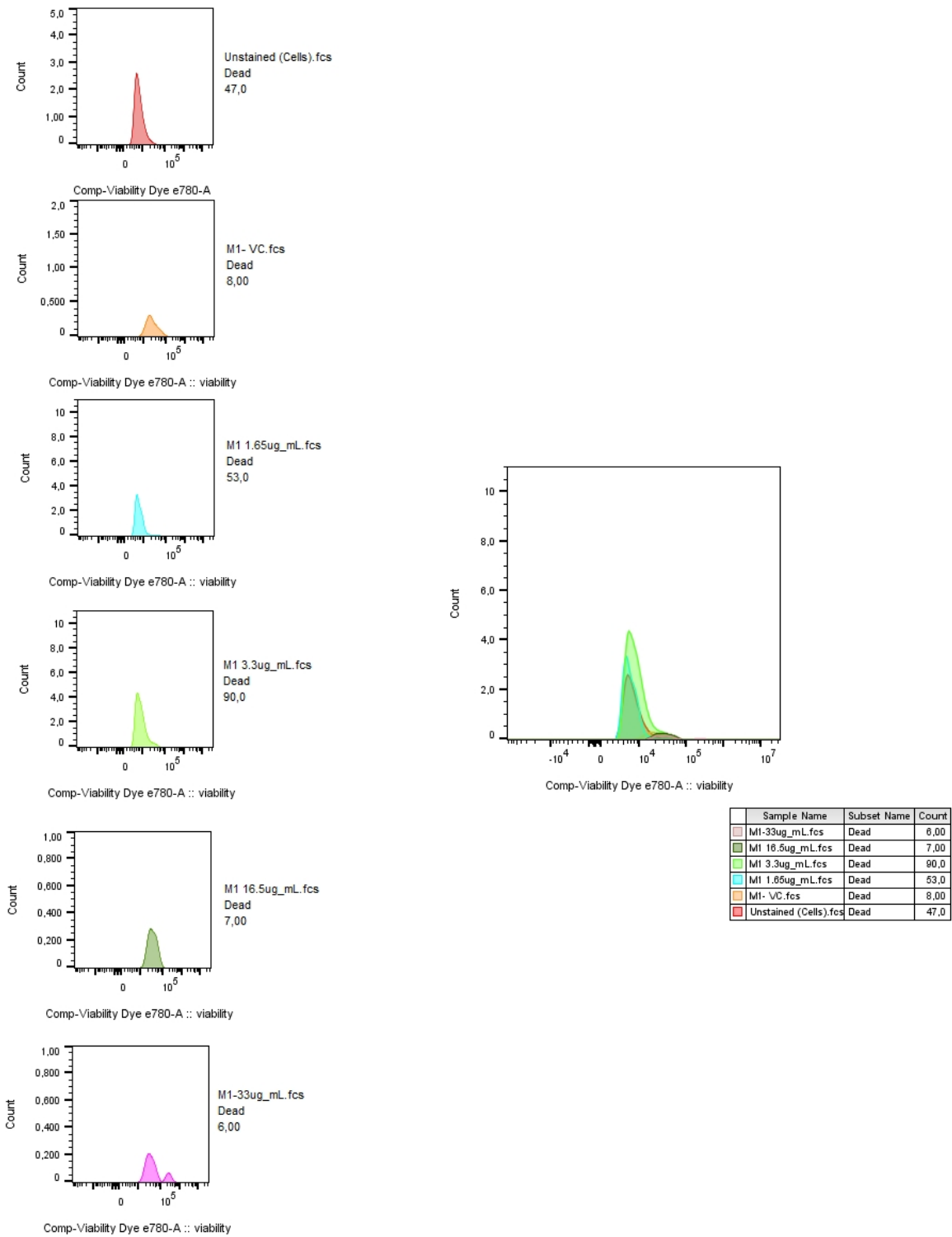
Figure 4.15: M1 macrophage viability.
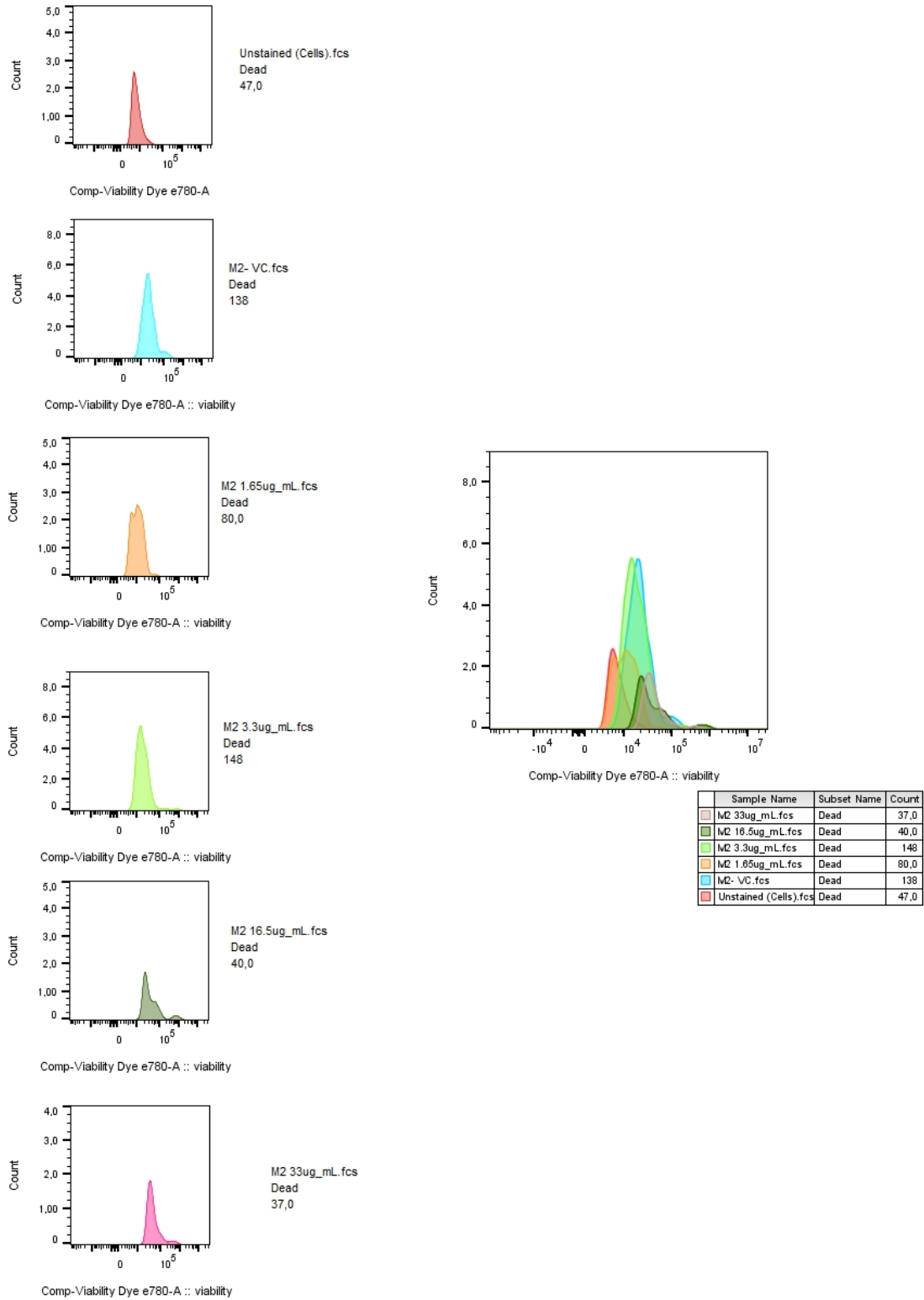
Figure 4.16: M2 macrophage viability.

51
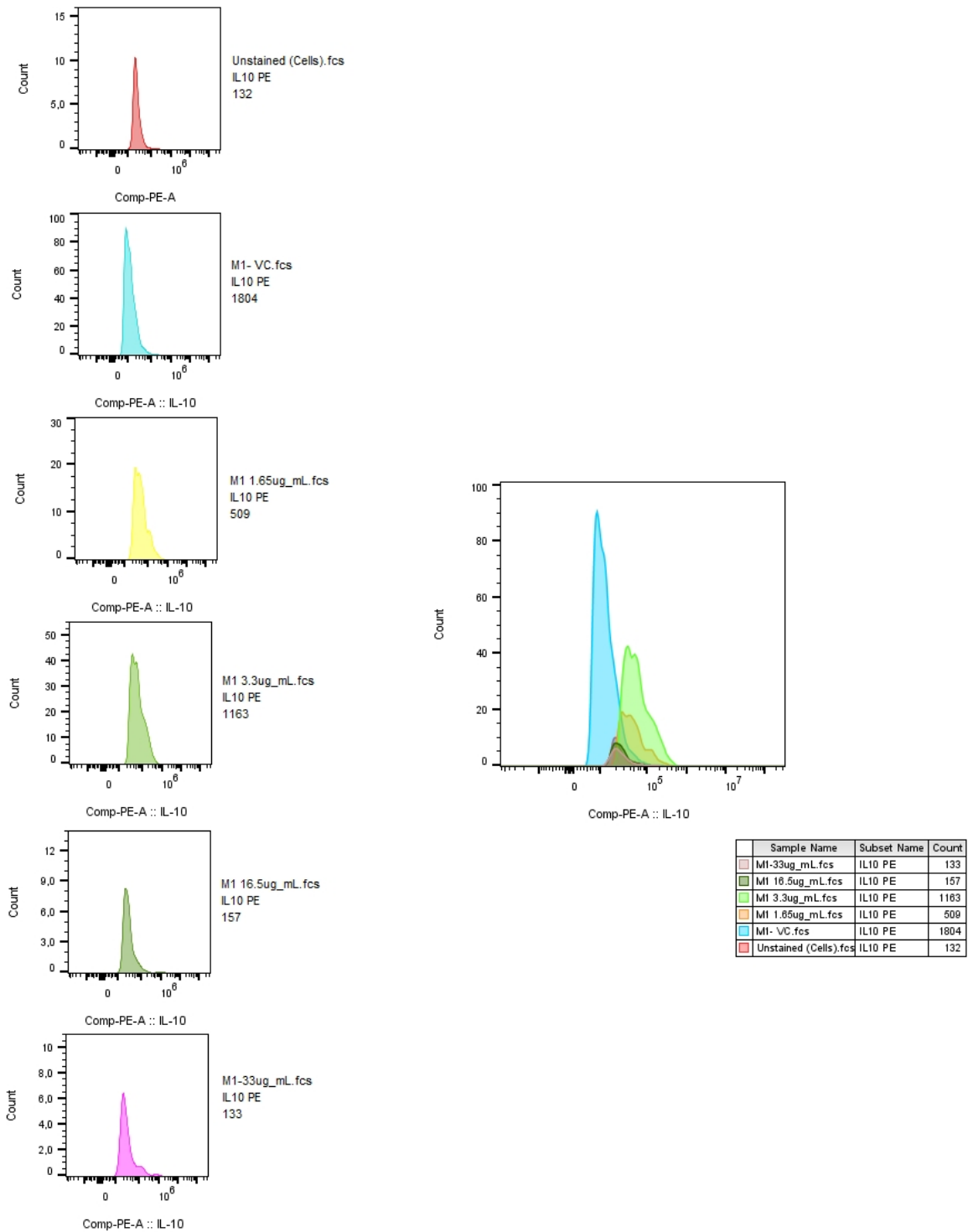
Figure 4.17: M1 Macrophage IL-10 expression. *This figure represents intracellular IL-10 expression in M1 polarized macrophages treated with various concentrations of DTG.*
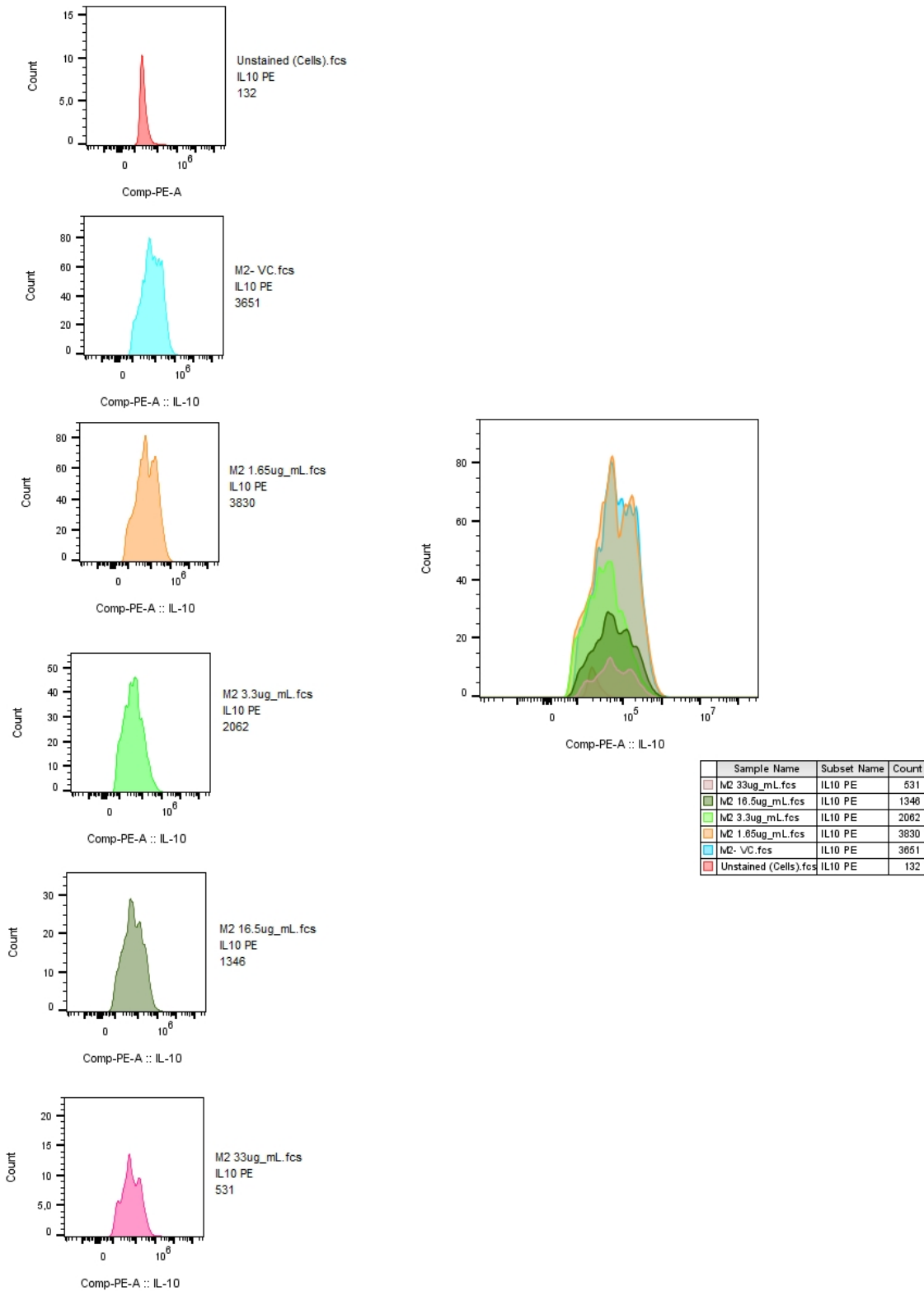
Figure 4.18: M2 Macrophage IL-10 expression. *This figure represents intracellular IL-10 expression in M2 polarized macrophages treated with various concentrations of DTG.*

Chapter 5: Discussion and conclusion

Discussion

The main aim of this study was to investigate the potential effect that DTG may have on the AT health profile in terms of inflammatory signalling, by conducting a 12-week treatment intervention study mimicking chronic DTG use in both male and female Wistar rats. We aimed to assess the cytokine profile and levels of fibrosis in the retroperitoneal AT depot - a visceral AT depot – in response to chronic DTG administration.

In contrast to reports of weight gain in patients after administration of DTG-containing ARV regimens[33,46,145,146], current data suggests that long-term DTG administration – in the absence of retroviral infection - does not result in weight gain, as indicated by both total body mass and retroperitoneal AT mass (Fig. 4.2 & Fig 4.3c). The mass of brain tissue was also compared as the brain is also an organ with high fat content and – just like AT - serves as a major viral reservoir. [6,10,147] In addition, neuropsychiatric adverse events are commonly reported in DTG-containing ARV regimens.[40,41,43] Again, no significant effect of DTG was observed (Fig. 4.3c).

There are few possible explanations as to why weight gain was not observed. This study was conducted without the confounder of HIV infection or cART. Previous animal studies reporting weight gain most commonly, but not exclusively, administered DTG-containing cARTs with or without the presence of SIV or HIV infection. It has previously been illustrated that the retrovirus itself and related viral proteins (e.g. Vpr, Tat and Nef) alter AT homeostasis. Amongst other effects, HIV viral proteins antagonise or supress PPARγ expression at mRNA and protein level – this will impair adipocyte differentiation and ultimately inhibit adipocyte hyperplasia.[10,101,148] A previous study illustrated DTG-containing cART treatment of SIV infected macaques were associated with increased PPARγ expression in both SAT and VAT depots[126] – this implies that cART appears to combat the effects that the retrovirus and related proteins have on a component of a very complex and integrated process. Although, there is still no clear indication of the effects that DTG in isolation and cART has on AT without the confounder of any retroviral infections – as the SIV infected cART animals were compared to untreated, uninfected controls. Thus, weight gain previously observed might potentially be ascribed to drug-virus interactions and/or drug-drug interaction.

In addition, HIV infections are widely associated with weight loss – this results from multiple consequences directly related to the retroviral infection. One commonly reported symptom of

HIV infection is the lack of appetite.[149] On average PLWH have increased energy expenditure – approximately 10 to 35% higher compared to HIV negative individuals.[150] More advanced HIV infections also alter the individual's ability to sufficiently absorb, store and utilise nutrients[151] as a result of diarrhoea, nausea and altered gut integrity caused by HIV.[149] One commonly self-reported effect of DTG-based cARTs is an increased appetite - allowing for an increased calorie consumption in order to overcome the increased energy expenditure. Other HIV related symptoms might also be alleviated by the use or DTG-based ARTs suggesting that individuals consume more when their adverse effects subside.

Lastly, it is possible that adipose health can be compromised without changes in adipose volume. That is why it is important to investigate cytokine profiles and other signs of accelerated aging – such as fibrosis[28] –that could be indicative of an adverse outcome.

In general, it is considered that females have a higher percentage of body fat compared to males.[152] This is thought to be as a result of sex hormones – with testosterone promoting an increase in muscle mass and estrogen favouring adipose deposition. [152] Upon ageing, there is a general decrease in testosterone levels that result in a relative increase in adiposity in males too.[152] In males, AT is mainly deposited in the visceral AT depots whereas in females, the AT is mainly subcutaneous.[153] Due to the documented sex differences, differences in the size of more visceral fat stores may have been expected, but our data demonstrated that there are no significant differences in the size of retroperitoneal AT depots. (Fig. 4.3. c) The retroperitoneal AT depot contributes only a small portion of the total visceral adiposity and for this reason no firm conclusions can be drawn in the absence of quantification of other visceral depots. Of relevance, a previous study aimed to investigate the sex-related differences in AT expansion of male and female Wistar rats reported marked differences in the contribution to percentage body weight that the retroperitoneal AT accounts for. The animals had unlimited access to standard chow and at 3 and 7 months of age the male retroperitoneal AT made up a higher portion of the animal body mass compared to the females.[154]

It is a well-known fact that body size of male animals are significantly larger than females.[140,152] The brain mass (when expressed relative to body mass) was significantly larger in females when compared to males. Data like this, highlights the need for the inclusion of both male and female animals in research, as a number of other sex-specific differences were also observed in the current study. Therefore, in order to facilitate a comparison of the

AT cytokine profiles between the males and females, cytokine levels were corrected for both body mass and retroperitoneal AT mass, as this in my opinion allowed for a more accurate representation of the secretory profile in the different sex groups.

When considering the adipokine profile of the visceral AT, one key observation made was that the female animals (control and treated) presented with higher levels of adiponectin and smaller adipocyte size[155] – both thought to be associated with favourable metabolic outcomes. [156–158] Adiponectin, an insulin-sensitising hormone with anti-atherogenic and anti-inflammatory properties is mainly secreted by AT.[159] It is the best known and most abundant adipokine found in human serum.[81] Research indicates that adiponectin presents with gender specific trends, with higher levels secreted in females compared to males[80] – similar results were obtained in our data (Fig. 4.6 a,b).Likewise, adipocyte size also presents with gender specific trends.

AT in males tend to expand through adipocyte hypertrophy, whereas adipocyte hyperplasia is the preferential means of expansions in females[154,160–162] – independent of adiposity.[163] Hypertrophic adipocytes are associated with a decrease in adiponectin secretion, hypoxia[164], fibrosis[111], increased immune cell infiltrations and increased levels of pro-inflammatory cytokines[165]. The contrary is true for hyperplasia – which is associated with increased adiponectin, sufficient vascularization, and the presence of other anti-inflammatory mediators. This is in line with the relatively higher adiponectin and smaller adipocyte size observed in the female AT.

Our data confirms that females tend to have smaller adipocytes when considering average adipocyte size in relation to body mass. It has previously been illustrated that adipocytes in males (abdominal and omental depots) reach maximum cell size at lower body mass indices compared to females.[160] Hypertrophy is associated with increased risk of insulin resistance and type II diabetes mellitus[166] – regardless of the region in which the AT is deposited.[160] Increased VAT increases the likelihood of adipocyte hypertrophy – although cells in female AT remains smaller compared to that of males. Even though, we compared adipocyte size between males and females in a cross-sectional design may we cannot give an accurate indication whether the adipocytes underwent hypertrophy or hyperplasia. However, when considering the effect of DTG treatment, a general (but not statistically significant) trend of decreased adipocyte size in the DTG-treated groups was observed compared to the control

groups. To my knowledge gender specific adipocyte size differences in response to DTG treatment has not previously been studied.

Hyperplasia can be considered as an adaptive measure – it has been suggested that there is a relationship between hyperplasia and hypertrophy of adipocytes. It is thought that there is an 'expansion threshold' and once this is reached, hyperplasia is induced. Hypertrophic adipocytes secrete a variety of paracrine factors which in turn recruits and stimulates proliferation of fibroblast-like progenitor cells to form preadipocytes and later differentiate into mature adipocytes[71,167] This process results in the formation of new, smaller adipocytes and is referred to as hyperplasia. Following this rationale, it is expected that an increase in cell numbers would be followed by an increase in cell size. These newly differentiated cells in turn are able to undergo significant expansions contributing to hypertrophic potential.[71] It is thought that this is an adaptive measure to combat the consequences that ensues once cells become hypertrophic.

This theory is potentially supported by considering the observations previously made in other studies and adipocyte morphology observed in our study. As previously mentioned, there was adipocyte hypertrophy and increased fibrosis observed after a 2-week treatment period[12,131] – this can be as a result of the initial hypertrophic expansion before the 'expansion threshold' is reached. Another study – conducted over a period of more than 2 years[126] – also reported adipocyte hypertrophy and increased AT fibrosis. Both these studies complement the data we generated. This implies that the duration of treatment in our study was sufficient to induce DTG associated AT outcomes. Following our 3-month treatment period - smaller cell sizes and low levels of fibrosis was reported - suggesting this might be an intermediate timepoint were the cells reached the 'expansion threshold' and adipocyte hyperplasia was induced. Without any confounders inducing or contributing to chronic inflammation and/or AT dysfunction the AT expansion has the potential to expand by following trends of intermitted periods of hyperplasia and hypertrophy. Whereas the other studies evaluating the effect of DTG on AT included the confounders of either cARTs and/or HIV or SIV infection – these factors have the potential of contributing to a chronic low-grade inflammatory state and promotes AT dysfunction.

A mouse study that aimed to assess the effects of DTG on various parameters including the AT of female C57BL6J mice – administered DTG subcutaneously over a treatment period of 2

weeks. During the course of the study a slight decrease in oxygen consumption and significant weight gain was observed. UCP1 expression in intrascapular VAT and inguinal WAT was reduced while SREBP, the master regulator of lipid synthesis, was upregulated in inguinal WAT and unchanged in BAT. The study suggests that DTG treatment disrupts energy balance by supressing energy expenditure in addition to resulting in decreased UCP 1 expression and mitochondrial disruption. However, I am of the opinion that the administration vehicle might in part be responsible for the effects observed. [131]

Previous studies illustrated elevated PPARγ activity in VAT of SIV infected-[126] and uninfected-[12] macaques treated with DTG-containing combination therapy. PPARγ is known as the master regulator of adipogenesis and responsible for adipocyte differentiation and lipid metabolism. One of the most important downstream effects of increased PPARγ is the activation of the transcription factor CCAAT/enhancer-binding protein-α (C/EBPα)[168,169] – together these two transcriptional factors take part in a positive feedback loop to maintain adipocyte differentiation (whereas impaired adipogenesis and AT dysfunction are associated with decreased levels of PARRγ)[170].

Transient inflammation is likely required for homeostatic functioning and expansion of AT[71,169] - although there are conflicting views.[171,172] It is thought that short periods of acute inflammation is required to drive adipocyte hyperplasia, also referred to as adipogenesis.[71] The process of adipogenesis is highly dependent on the crosstalk between the adipocytes and other cellular components and/or the surrounding ECM.

AT in the current study exhibited very low levels of fibrosis, suggesting that ECM was not significantly dysregulated in the current study. However, when considering the pro-inflammatory markers, both TNFα and MCP-1 levels were higher in the females compared to males, although only reaching statistical significance in the DTG-treated groups. One possible explanation for the elevated TNF-a and MCP-1 in the female AT is the female pro-inflammatory bias – a phenomenon that females have an increased tendency for inflammation.[173]. Interestingly in males, the TNFα levels were further depressed in the DTG-treated group when compared to the control, while in contrast, the DTG-treated females presented with higher levels compared to the female controls. This potentially suggests exacerbated inflammation or inflammatory response to DTG in the females only.

This relatively more pro-inflammatory state in females, together with the observed adipocyte hyperplasia, may explain why previous studies illustrated increased incidence of weight gain in females. We suggest AT homeostatic control of hyperplasia and hypertrophy is altered by a combination of; increased cell numbers brought about by adipocyte hyperplasia, low-grade inflammation induced by the HIV infection itself and the potentiating effects of DTG containing ARV regimens. The concurrent production of new cells, combined with and the expansion potential of these cells i.e., hypertrophy - contributes to AT dysfunction and chronic inflammation.

Macrophages play a prominent role in inflammation - when probing the macrophage phenotypes- the trends of CD68, regarded as a M1 macrophages marker[174], and intracellular IL-10, a cytokine with potent anti-inflammatory properties[175], data suggests that DTG may induce anti-inflammatory effects at lower concentrations whereas higher concentrations are associated with a more pro-inflammatory phenotype. The relevance of this finding should be tested in a larger *in vitro* study as well as *in vivo*, and in particular in adipose-associated macrophages. Currently there are conflicting views on whether there is a relatively increased clearance of DTG from AT, or accumulation[9,147] . The dose-specificity suggested by our preliminary data in macrophages in culture – albeit premature – suggests the importance of elucidating DTG levels in adipose, as this may significantly impact on AT inflammatory profile. This provides evidence that further investigation is needed to shed light on the DTG bioavailability and potential accumulation in AT to fully elucidate its effects.

It is hypothesized that under normal physiological conditions a balance exists between adipocyte hyperplasia and adipocyte hypertrophy.[176] Adipocytes undergo slight expansion by means of hypertrophy until a hypertrophic 'threshold' in reached. This results in the accumulation ROS and an acute inflammatory response which fuels adipocyte hyperplasia. This in turn alleviates hypertrophy as the increased cell number alleviates the increased storage demands brought about by instances such as periods of excess energy consumption. Hyperplasia is also associated with ECM remodelling, which successively is associated with inflammation[177]. Furthermore, adipocyte differentiation itself is associated with increased mitochondrial metabolism (and thus ROS production) [71,169,178]. Finally, in the context of DTG, if left unchecked, the self-perpetuating loop, increased ROS and low-grade inflammation may

result in chronic unresolved inflammation and ultimately AT dysfunction, as illustrated in Fig. 5.1.
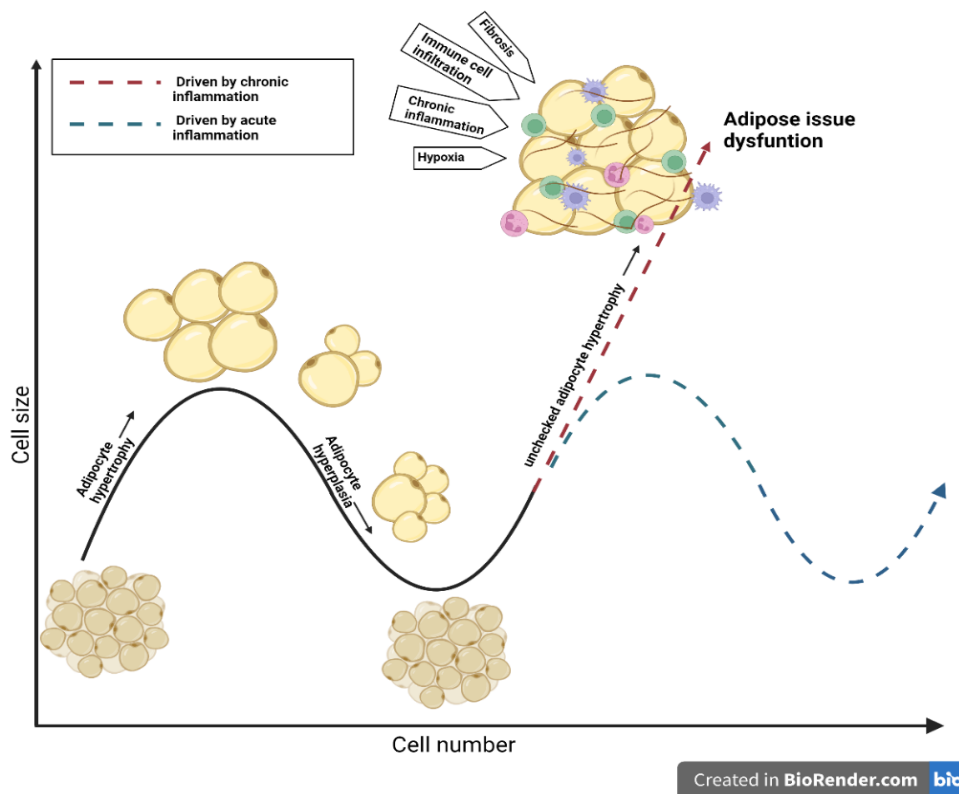
Figure 5.1: Adipose tissue expansion

Thus, to elaborate on the mechanisms at play, I would suggest that future studies assess cytokine, adipokine profiles, as well as parameters of redox status longitudinally. This could indicate if the increased pro-inflammatory cytokines profiles are only occurring in females in response to DTG, as well as to elucidate whether males may be relatively more protected by potential protective mechanisms – e.g. antioxidant counter-mechanisms.

Although multiple studies recently conducted advised against prescribing DTG as monotherapy as there are reported increased incidences of virological failure and emergence of drug resistance. Despite these advisements, it is still necessary to conduct studies on DTG in isolation in order to probe and fully understand the effects that it imposes when administered insolation.

Limitations to the study include not tracking the estrous cycle of the female rodents as some of the cytokine levels fluctuated thought the course of the cycle. As there are differences in the patterns in which AT are deposited in males and females – in part driven by the sex

hormones - it is expect that there are changes in the AT as a result of fluctuation of hormones that occur throughout the course of the estrous cycle. There are contradicting views on adiponectin levels and estrous cycle associated fluctuation. Previous studies have illustrated that adiponectin fluctuate throughout the menstrual cycle.[179,180] Whereas others suggests that adiponectin levels remain stable.[181] Estrogen also plays a major role in adipogenesis and AT metabolism- suggesting that estrogen can in part be the reason why smaller cell sizes are observed in female AT.[182]

Another suggestion would be to include different AT depots – to i) give a more accurate representation of the visceral adiposity of the animals and ii) include subcutaneous AT as there are marked sex differences previously reported. Furthermore, a parallel study is suggested to assess the changes in various AT depots including the subcutaneous and other visceral AT depots. This would allow the conclusions to be drawn on the observation in the subcutaneous AT depots and how that correlate to changes in visceral AT. As subcutaneous AT is more readily and easily accessible in when considering human studies, it is important to investigate the similarities and differences in the way these AT depots have in response to dolutegravir treatment. Previous studies illustrated that the subcutaneous AT are also affected by DTG treatment. In these studies, increased PARRγ expression, increased adipocyte size in fibrosis were illustrated.

The relatively small sample size – though adequate for assessment of tissue profiles – did not allow for assessment of circulating levels of adipokines and cytokines. Including these measures may facilitate the extrapolation of pre-clinical model data to the human clinical situation. This would allow further insight on the effects that DTG have on whole body vs AT adipokine and pro-inflammatory profiles.

Conclusion

Current data illustrates that in terms of potential effects of dolutegravir on AT health, females seem more vulnerable to undesired longer term outcome. The overall small effect sizes seen is in line with a chronic, low-grade dysregulation which may predispose dolutegravir-treated patients to development of co-morbidities with a chronic inflammatory character.

The generated data confirms that highlights the female bias to negative adverse events from DTG administration as suggested from literature. This warrants the inclusion of both males and females in future research investigating DTG.

Bibliography

1.   United Nations Programme on HIV/aids. UNAIDS. UNAIDS data 2021. 4–38 (2021).

2.   Couturier, J. & Lewis, D. E. HIV Persistence in Adipose Tissue Reservoirs. *Curr. HIV/AIDS Rep.* **15**, 60–71 (2018).

3.   Castellano, P., Prevedel, L., Valdebenito, S. & Eugenin, E. A. HIV infection and latency induce a unique metabolic signature in human macrophages. *Sci. Rep.* **9**, 1–14 (2019).

4.   Hendricks, C. M., Cordeiro, T., Gomes, A. P. & Stevenson, M. The Interplay of HIV-1 and Macrophages in Viral Persistence. *Front. Microbiol.* **12**, 1–15 (2021).

5.   Couturier, J. *et al.* Adipocytes impair efficacy of antiretroviral therapy. *Antiviral Res.* **154**, 140–148 (2018).

6.   Wong, J. K. & Yukl, S. A. Tissue reservoirs of HIV. *Curr. Opin. HIV AIDS* **11**, 362–370 (2016).

7.   Gelé, T. *et al.* Characteristics of dolutegravir and bictegravir plasma protein binding: A first approach for the study of pharmacologic sanctuaries. *Antimicrob. Agents Chemother.* **64**, 1–4 (2020).

8.   Siliciano, R. F. & Greene, W. C. HIV latency. *Cold Spring Harb. Perspect. Med.* **1**, 1–19 (2011).

9.   Labarthe, L. *et al.* Pharmacokinetics and tissue distribution of tenofovir, emtricitabine and dolutegravir in mice. *J. Antimicrob. Chemother.* 1–8 (2022) doi:10.1093/jac/dkab501.

10.   Damouche, A. *et al.* Adipose Tissue Is a Neglected Viral Reservoir and an Inflammatory Site during Chronic HIV and SIV Infection. *PLoS Pathog.* **11**, 1–28 (2015).

11.   Eckard, A. R. & McComsey, G. A. Weight gain and integrase inhibitors. *Curr. Opin.*

Infect. Dis. **33**, 10–19 (2020).

12. Gorwood, J. *et al.* The integrase inhibitors dolutegravir and raltegravir exert proadipogenic and profibrotic effects and induce insulin resistance in human/simian adipose tissue and human adipocytes. *Clin. Infect. Dis.* **71**, E549–E560 (2020).

13. Giacomet, V. *et al.* Body Fat Distribution and Metabolic Changes in a Cohort of Adolescents Living with HIV Switched to an Antiretroviral Regimen Containing Dolutegravir. *Pediatr. Infect. Dis. J.* **40**, 457–459 (2021).

14. Gorwood, J. *et al.* The Integrase Inhibitors Dolutegravir and Raltegravir Exert Proadipogenic and Profibrotic Effects and Induce Insulin Resistance in Human/Simian Adipose Tissue and Human Adipocytes. *Clin. Infect. Dis.* **71**, e549–e560 (2020).

15. Kralova Lesna, I. *et al.* Characterisation and comparison of adipose tissue macrophages from human subcutaneous, visceral and perivascular adipose tissue. *J. Transl. Med.* **14**, 1–9 (2016).

16. Janochova, K., Haluzik, M. & Buzga, M. Visceral fat and insulin resistance – what we know? *Biomed. Pap.* **163**, 19–27 (2019).

17. Thomas, D. & Apovian, C. Macrophage functions in lean and obese adipose tissue. *Metabolism* **72**, 120–143 (2017).

18. Corona-Meraz, F.-I. *et al.* Adipose Tissue in Health and Disease. in *Obesity* vol. 176 139–148 (IntechOpen, 2020).

19. D'Alessandro, M. E., Selenscig, D., Illesca, P., Chicco, A. & Lombardo, Y. B. Time course of adipose tissue dysfunction associated with antioxidant defense, inflammatory cytokines and oxidative stress in dyslipemic insulin resistant rats. *Food Funct.* **6**, 1299–1309 (2015).

20. Gálvez, I. *et al.* The Influence of Obesity and Weight Loss on the Bioregulation of Innate/Inflammatory Responses: Macrophages and Immunometabolism. *Nutrients* **14**, (2022).

21. Unamuno, X. *et al.* Adipokine dysregulation and adipose tissue inflammation in human obesity. *Eur. J. Clin. Invest.* **48**, 1–11 (2018).

22. Acosta, J. R. *et al.* Human-Specific Function of IL-10 in Adipose Tissue Linked to Insulin Resistance. *J. Clin. Endocrinol. Metab.* **104**, 4552–4562 (2019).

23. Lindhorst, A. *et al.* Adipocyte death triggers a pro-inflammatory response and induces metabolic activation of resident macrophages. *Cell Death Dis.* **12**, (2021).

24. Thomas, D. & Apovian, C. Macrophage functions in lean and obese adipose tissue. *Metabolism* **72**, 120–143 (2017).

25. Pellegrinelli, V., Carobbio, S. & Vidal-Puig, A. Adipose tissue plasticity: how fat depots respond differently to pathophysiological cues. *Diabetologia* **59**, 1075–1088 (2016).

26. Russo, L. & Lumeng, C. N. Properties and functions of adipose tissue macrophages in obesity. *Immunology* **155**, 407–417 (2018).

27. Pérez, L. M. *et al.* 'Adipaging': ageing and obesity share biological hallmarks related to a dysfunctional adipose tissue. *J. Physiol.* **594**, 3187–3207 (2016).

28. Ross, K. S. & Smith, C. D-Galactose: a Model of Accelerated Ageing Sufficiently Sensitive To Reflect Preventative Efficacy of an Antioxidant Treatment. *Biogerontology* **21**, 745–761 (2020).

29. Ollewagen, T., Myburgh, K. H., van de Vyver, M. & Smith, C. Rheumatoid cachexia: the underappreciated role of myoblast, macrophage and fibroblast interplay in the skeletal muscle niche. *J. Biomed. Sci.* **28**, 1–16 (2021).

30. Fantauzzi, A. & Mezzaroma, I. Dolutegravir: Clinical efficacy and role in HIV therapy. *Ther. Adv. Chronic Dis.* **5**, 164–177 (2014).

31. South African National Department of Health. 2019 ART Clinical Guidelines. (2019).

32. Kandel, C. E. & Walmsley, S. L. Dolutegravir – A review of the pharmacology, efficacy, and safety in the treatment of HIV. *Drug Des. Devel. Ther.* **9**, 3547–3555 (2015).

33. Taramasso, L. *et al.* Factors associated with weight gain in people treated with dolutegravir. *Open Forum Infect. Dis.* **7**, 1–8 (2020).

34. Hirigo, A. T., Gutema, S., Eifa, A. & Ketema, W. Experience of dolutegravir-based antiretroviral treatment and risks of diabetes mellitus. *SAGE Open Med. Case Reports* **10**, 2050313X2210794 (2022).

35. Phillips, A. N. *et al.* Risks and benefits of dolutegravir-based antiretroviral drug regimens in sub-Saharan Africa: a modelling study. *Lancet HIV* **6**, e116–e127 (2019).

36. Hocqueloux, L. *et al.* Dolutegravir Monotherapy Versus Dolutegravir/Abacavir/Lamivudine for Virologically Suppressed People Living with Chronic Human Immunodeficiency Virus Infection: The Randomized Noninferiority MONotherapy of TiviCAY Trial. *Clin. Infect. Dis.* **69**, 1498–1505 (2019).

37. Phillips, A. N. *et al.* Updated assessment of risks and benefits of dolutegravir versus efavirenz in new antiretroviral treatment initiators in sub-Saharan Africa: modelling to inform treatment guidelines. *Lancet HIV* **7**, e193–e200 (2020).

38. Wijting, I. *et al.* Dolutegravir as maintenance monotherapy for HIV (DOMONO): a phase 2, randomised non-inferiority trial. *Lancet HIV* **4**, e547–e554 (2017).

39. Blanco, J. L. *et al.* Dolutegravir-based maintenance monotherapy versus dual therapy with lamivudine: A planned 24 week analysis of the DOLAM randomized clinical trial. *J. Antimicrob. Chemother.* **73**, 1965–1971 (2018).

40. Hoffmann, C. & Llibre, J. M. Neuropsychiatric adverse events with dolutegravir and other integrase strand transfer inhibitors. *AIDS Rev.* **21**, 4–10 (2019).

41. Kolakowska, A., Maresca, A. F., Collins, I. J. & Cailhol, J. Update on Adverse Effects of HIV Integrase Inhibitors. *Curr. Treat. Options Infect. Dis.* **11**, 372–387 (2019).

42. Aboud, M. *et al.* Dolutegravir versus ritonavir-boosted lopinavir both with dual nucleoside reverse transcriptase inhibitor therapy in adults with HIV-1 infection in whom first-line therapy has failed (DAWNING): an open-label, non-inferiority, phase 3b trial. *Lancet Infect. Dis.* **19**, 253–264 (2019).

43. Administration, T. G. AusPAR Attachment 2 Extract from the Clinical Evaluation Report for mirabegron Proprietary Product Name : Betmiga. (2013).

44. Wu, J., Wu, H., Lu, C., Guo, L. & Li, P. Self-reported sleep disturbances in HIV-infected people: A meta-analysis of prevalence and moderators. *Sleep Med.* **16**, 901–907 (2015).

45. Koethe, J. R. *et al.* Adipokines, Weight Gain and Metabolic and Inflammatory Markers

After Antiretroviral Therapy Initiation: AIDS Clinical Trials Group (ACTG) A5260s. *Clin. Infect. Dis.* **37232**, 1–8 (2021).

46. Sax, P. E. *et al.* Weight gain following initiation of antiretroviral therapy: Risk factors in randomized comparative clinical trials. *Clin. Infect. Dis.* **71**, 1379–1389 (2020).

47. Lake, J. E. & Currier, J. S. Metabolic disease in HIV infection. *Lancet Infect. Dis.* **13**, 964–975 (2013).

48. Bourgi, K. *et al.* Greater Weight Gain in Treatment-naive Persons Starting Dolutegravir-based Antiretroviral Therapy. *Clin. Infect. Dis.* **70**, 1267–1274 (2020).

49. Griesel, R. *et al.* Concentration–response relationships of dolutegravir and efavirenz with weight change after starting antiretroviral therapy. *Br. J. Clin. Pharmacol.* **88**, 883–893 (2022).

50. Calcagno, A. *et al.* Older Age is Associated with Higher Dolutegravir Exposure in Plasma and Cerebrospinal Fluid of People Living with HIV. *Clin. Pharmacokinet.* **60**, 103–109 (2021).

51. Kandel, C. E. & Walmsley, S. L. Dolutegravir – A review of the pharmacology, efficacy, and safety in the treatment of HIV. *Drug Des. Dev. Ther. (1).pdf* **9**, 3547–3555 (2015).

52. Cahn, P. *et al.* Dolutegravir versus raltegravir in antiretroviral-experienced, integrase-inhibitor-naive adults with HIV: Week 48 results from the randomised, double-blind, non-inferiority SAILING study. *Lancet* **382**, 700–708 (2013).

53. Clotet, B. *et al.* Once-daily dolutegravir versus darunavir plus ritonavir in antiretroviral-naive adults with HIV-1 infection (FLAMINGO): 48 week results from the randomised open-label phase 3b study. *Lancet* **383**, 2222–2231 (2014).

54. Moss, L. *et al.* The comparative disposition and metabolism of dolutegravir, a potent HIV-1 integrase inhibitor, in mice, rats, and monkeys. *Xenobiotica* **45**, 60–70 (2015).

55. Barcelo, C. *et al.* Population pharmacokinetics of dolutegravir: Influence of drug-drug interactions in a real-life setting. *J. Antimicrob. Chemother.* **74**, 2690–2697 (2019).

56. Zhu, J. *et al.* CYP1A1 and 1B1-mediated metabolic pathways of dolutegravir , an HIV integrase inhibitor. *Biochem. Pharmacol.* **158**, 174–184 (2018).

57.   Taha, H., Das, A. & Das, S. Clinical effectiveness of dolutegravir in the treatment of HIV/AIDS. *Infect. Drug Resist.* **8**, 339–352 (2015).

58.   Podany, A. T., Scarsi, K. K. & Fletcher, C. V. Comparative Clinical Pharmacokinetics and Pharmacodynamics of HIV-1 Integrase Strand Transfer Inhibitors. *Clin. Pharmacokinet.* **56**, 25–40 (2017).

59.   European Medicines Agency. Tivicay Assessment Report. **44**, (2013).

60.   Letendre, S. L. *et al.* ING116070: A study of the pharmacokinetics and antiviral activity of dolutegravir in cerebrospinal fluid in HIV-1-infected, antiretroviral therapy-naive subjects. *Clin. Infect. Dis.* **59**, 1032–1037 (2014).

61.   Dupin, N. *et al.* HIV and antiretroviral drug distribution in plasma and fat tissue of HIV-infected patients with lipodystrophy. *Aids* **16**, 2419–2424 (2002).

62.   Parant, F., Miailhes, P., Brunel, F. & Gagnieu, M. C. Dolutegravir Population Pharmacokinetics in a Real-Life Cohort of People Living with HIV Infection: A Covariate Analysis. *Ther. Drug Monit.* **41**, 444–451 (2019).

63.   Bourgeois, C. *et al.* Contribution of Adipose Tissue to the Chronic Immune Activation and Inflammation Associated With HIV Infection and Its Treatment. *Front. Immunol.* **12**, 1–22 (2021).

64.   Suganami, T. & Ogawa, Y. Adipose tissue macrophages: their role in adipose tissue remodeling. *J. Leukoc. Biol.* **88**, 33–39 (2010).

65.   Bourgeois, C. *et al.* Specific Biological Features of Adipose Tissue, and Their Impact on HIV Persistence. *Front. Microbiol.* **10**, 1–25 (2019).

66.   Li, Y., Yun, K. & Mu, R. A review on the biology and properties of adipose tissue macrophages involved in adipose tissue physiological and pathophysiological processes. *Lipids Health Dis.* **19**, 1–9 (2020).

67.   Koethe, J. R. *et al.* HIV and antiretroviral therapy-related fat alterations. *Nat. Rev. Dis. Prim.* **6**, (2020).

68.   Reilly, S. M. & Saltiel, A. R. Adapting to obesity with adipose tissue inflammation. *Nat. Rev. Endocrinol.* **13**, 633–643 (2017).

69. Marcelin, G., Silveira, A. L. M., Martins, L. B., Ferreira, A. V. M. & Clément, K. Deciphering the cellular interplays underlying obesityinduced adipose tissue fibrosis. *J. Clin. Invest.* **129**, 4032–4040 (2019).

70. Valencak, T. G., Osterrieder, A. & Schulz, T. J. Sex matters: The effects of biological sex on adipose tissue biology and energy metabolism. *Redox Biol.* **12**, 806–813 (2017).

71. Ghaben, A. L. & Scherer, P. E. Adipogenesis and metabolic health. *Nat. Rev. Mol. Cell Biol.* **20**, 242–258 (2019).

72. Pyrina, I. *et al.* Fate of Adipose Progenitor Cells in Obesity-Related Chronic Inflammation. *Front. Cell Dev. Biol.* **8**, 1–8 (2020).

73. Zoico, E. *et al.* Brown and beige adipose tissue and aging. *Front. Endocrinol. (Lausanne).* **10**, 1–10 (2019).

74. Villarroya, F., Cereijo, R., Gavaldà-Navarro, A., Villarroya, J. & Giralt, M. Inflammation of brown/beige adipose tissues in obesity and metabolic disease. *J. Intern. Med.* **284**, 492–504 (2018).

75. Ruggiero, A. D., Key, C. C. C. & Kavanagh, K. Adipose Tissue Macrophage Polarization in Healthy and Unhealthy Obesity. *Front. Nutr.* **8**, 1–14 (2021).

76. Schoettl, T., Fischer, I. P. & Ussar, S. Heterogeneity of adipose tissue in development and metabolic function. *J. Exp. Biol.* **121**, (2018).

77. Chusyd, D. E., Wang, D., Huffman, D. M. & Nagy, T. R. Relationships between Rodent White Adipose Fat Pads and Human White Adipose Fat Depots. *Front. Nutr.* **3**, (2016).

78. Kwok, K. H. M., Lam, K. S. L. & Xu, A. Heterogeneity of white adipose tissue: Molecular basis and clinical implications. *Exp. Mol. Med.* **48**, (2016).

79. Ruiz-Castell, M. *et al.* Estimated visceral adiposity is associated with risk of cardiometabolic conditions in a population based study. *Sci. Rep.* **11**, 1–9 (2021).

80. Chait, A. & den Hartigh, L. J. Adipose Tissue Distribution, Inflammation and Its Metabolic Consequences, Including Diabetes and Cardiovascular Disease. *Front. Cardiovasc. Med.* **7**, 1–41 (2020).

81. Mancuso, P. The role of adipokines in chronic inflammation. *ImmunoTargets Ther.* **5**,

47–56 (2016).

82. Chang, E., Varghese, M. & Singer, K. Gender and Sex Differences in Adipose Tissue. *Curr. Diab. Rep.* **18**, 69 (2018).

83. Shungin, D. *et al.* New genetic loci link adipose and insulin biology to body fat distribution. *Nature* **518**, 187–196 (2015).

84. Moreira-Pais, A. *et al.* Sex differences on adipose tissue remodeling: from molecular mechanisms to therapeutic interventions. *J. Mol. Med.* **98**, 483–493 (2020).

85. Li, C. *et al.* Macrophage polarization and meta-inflammation. *Transl. Res.* **191**, 29–44 (2018).

86. Ramakrishnan, V. M. & Boyd, N. L. The Adipose Stromal Vascular Fraction as a Complex Cellular Source for Tissue Engineering Applications. *Tissue Eng. - Part B Rev.* **24**, 289–299 (2018).

87. Abdelaziz, M. H. *et al.* Alternatively activated macrophages; A double-edged sword in allergic asthma. *J. Transl. Med.* **18**, 1–12 (2020).

88. Merino, K. M., Allers, C., Didier, E. S. & Kuroda, M. J. Role of monocyte/macrophages during HIV/SIV infection in adult and pediatric acquired immune deficiency syndrome. *Front. Immunol.* **8**, 1–16 (2017).

89. Smith, C., Kruger, M. J., Smith, R. M. & Myburgh, K. H. The inflammatory response to skeletal muscle injury: Illuminating complexities. *Sport. Med.* **38**, 947–969 (2008).

90. Cildir, G., Akincilar, S. C. & Tergaonkar, V. Chronic adipose tissue inflammation: All immune cells on the stage. *Trends Mol. Med.* **19**, 487–500 (2013).

91. Zhang, C., Yang, M. & Ericsson, A. C. Function of Macrophages in Disease: Current Understanding on Molecular Mechanisms. *Front. Immunol.* **12**, 1–12 (2021).

92. Biswas, S. K. & Mantovani, A. Orchestration of metabolism by macrophages. *Cell Metab.* **15**, 432–437 (2012).

93. Chambers, M. *et al.* Macrophage Plasticity in Reproduction and Environmental Influences on Their Function. *Front. Immunol.* **11**, 1–16 (2021).

94. Saeki, N. & Imai, Y. Reprogramming of synovial macrophage metabolism by synovial fibroblasts under inflammatory conditions. *Cell Commun. Signal.* **18**, 1–14 (2020).

95. Colin, S., Chinetti-Gbaguidi, G. & Staels, B. Macrophage phenotypes in atherosclerosis. *Immunol. Rev.* **262**, 153–166 (2014).

96. Zhou, D. *et al.* Promising landscape for regulating macrophage polarization: Epigenetic viewpoint. *Oncotarget* **8**, 57693–57706 (2017).

97. Zhu, L., Zhao, Q., Yang, T., Ding, W. & Zhao, Y. Cellular metabolism and macrophage functional polarization. *Int. Rev. Immunol.* **34**, 82–100 (2015).

98. Weagel, E., Smith, C., Liu, P. G., Robison, R. & Kim, O. Macrophage Polarization and Its Role in Cancer. *J. Clin. Cell. Immunol.* **06**, (2015).

99. Onogi, Y. *et al.* Pro-inflammatory macrophages coupled with glycolysis remodel adipose vasculature by producing platelet-derived growth factor-B in obesity. *Sci. Rep.* **10**, 1–13 (2020).

100. Diep Nguyen, T. Adiponectin: Role in physiology and pathophysiology. *Int. J. Prev. Med.* **11**, 136 (2020).

101. Gorwood, J. *et al.* Impact of HIV/simian immunodeficiency virus infection and viral proteins on adipose tissue fibrosis and adipogenesis. *Aids* **33**, 953–964 (2019).

102. Domingo, P. *et al.* Differential effects of raltegravir , dolutegravir and bictegravir on human adipocytes. 4923533.

103. Chen, L. *et al.* Inflammatory responses and inflammation-associated diseases in organs. *Oncotarget* **9**, 7204–7218 (2018).

104. Taouis, M. & Benomar, Y. Is resistin the master link between inflammation and inflammation-related chronic diseases? *Mol. Cell. Endocrinol.* **533**, 111341 (2021).

105. Tripathi, D., Kant, S., Pandey, S. & Ehtesham, N. Z. Resistin in metabolism, inflammation, and disease. *FEBS J.* **287**, 3141–3149 (2020).

106. Acquarone, E., Monacelli, F., Borghi, R., Nencioni, A. & Odetti, P. Resistin: A reappraisal. *Mech. Ageing Dev.* **178**, 46–63 (2019).

107. Akhter, N. *et al.* ROS/TNF-α crosstalk triggers the expression of IL-8 and MCP-1 in human monocytic THP-1 cells via the NF-κB and ERK1/2 mediated signaling. *Int. J. Mol. Sci.* **22**, (2021).

108. Singh, S., Anshita, D. & Ravichandiran, V. MCP-1: Function, regulation, and involvement in disease. *Int. Immunopharmacol.* **101**, 107598 (2021).

109. Li, S., Gao, H., Hasegawa, Y. & Lu, X. Fight against fibrosis in adipose tissue remodeling. *Am. J. Physiol. - Endocrinol. Metab.* **321**, E169–E175 (2021).

110. Choe, S. S., Huh, J. Y., Hwang, I. J., Kim, J. I. & Kim, J. B. Adipose tissue remodeling: Its role in energy metabolism and metabolic disorders. *Front. Endocrinol. (Lausanne).* **7**, 1–16 (2016).

111. Crewe, C., An, Y. A. & Scherer, P. E. The ominous triad of adipose tissue dysfunction: Inflammation, fibrosis, and impaired angiogenesis. *J. Clin. Invest.* **127**, 74–82 (2017).

112. Wynn, T. A. & Vannella, K. M. Macrophages in Tissue Repair, Regeneration, and Fibrosis. *Immunity* **44**, 450–462 (2016).

113. Pahwa, R., Goyal, A. & Jialal, I. *Chronic Inflammation. StatPearls* (2022).

114. Sun, K., Tordjman, J., Clément, K. & Scherer, P. E. Fibrosis and adipose tissue dysfunction. *Cell Metab.* **18**, 470–477 (2013).

115. Kawasaki, N., Asada, R., Saito, A., Kanemoto, S. & Imaizumi, K. Obesity-induced endoplasmic reticulum stress causes chronic inflammation in adipose tissue. *Sci. Rep.* **2**, 1–7 (2012).

116. Khan, S., Chan, Y. T., Revelo, X. S. & Winer, D. A. The Immune Landscape of Visceral Adipose Tissue During Obesity and Aging. *Front. Endocrinol. (Lausanne).* **11**, 1–18 (2020).

117. Klöting, N. & Blüher, M. Adipocyte dysfunction, inflammation and metabolic syndrome. *Rev. Endocr. Metab. Disord.* **15**, 277–287 (2014).

118. Petersen, K. S. & Smith, C. Ageing-associated oxidative stress and inflammation are alleviated by products from grapes. *Oxid. Med. Cell. Longev.* **2016**, (2016).

119. Pizzino, G. *et al.* Oxidative Stress: Harms and Benefits for Human Health. *Oxid. Med.*

Cell. Longev. **2017**, (2017).

120. Masschelin, P. M., Cox, A. R., Chernis, N. & Hartig, S. M. The Impact of Oxidative Stress on Adipose Tissue Energy Balance. *Front. Physiol.* **10**, 1–8 (2020).

121. Zhou, Y., Li, H. & Xia, N. The Interplay Between Adipose Tissue and Vasculature: Role of Oxidative Stress in Obesity. *Front. Cardiovasc. Med.* **8**, 1–14 (2021).

122. Debari, M. K. & Abbott, R. D. Adipose tissue fibrosis: Mechanisms, models, and importance. *Int. J. Mol. Sci.* **21**, 1–24 (2020).

123. Michailidou, Z. Fundamental roles for hypoxia signalling in adipose tissue metabolism and inflammation in obesity. *Curr. Opin. Physiol.* **12**, 39–43 (2019).

124. Lin, D., Chun, T. H. & Kang, L. Adipose extracellular matrix remodelling in obesity and insulin resistance. *Biochem. Pharmacol.* **119**, 8–16 (2016).

125. Ruiz-Ojeda, F. J., Méndez-Gutiérrez, A., Aguilera, C. M. & Plaza-Díaz, J. Extracellular matrix remodeling of adipose tissue in obesity and metabolic diseases. *Int. J. Mol. Sci.* **20**, (2019).

126. Ngono Ayissi, K. *et al.* Inhibition of Adipose Tissue Beiging by HIV Integrase Inhibitors, Dolutegravir and Bictegravir, Is Associated with Adipocyte Hypertrophy, Hypoxia, Elevated Fibrosis, and Insulin Resistance in Simian Adipose Tissue and Human Adipocytes. *Cells* **11**, 1841 (2022).

127. Sun, K. *et al.* Endotrophin triggers adipose tissue fibrosis and metabolic dysfunction. *Nat. Commun.* **5**, 3485 (2014).

128. Khan, T. *et al.* Metabolic Dysregulation and Adipose Tissue Fibrosis: Role of Collagen VI. *Mol. Cell. Biol.* **29**, 1575–1591 (2009).

129. Li, X. *et al.* Critical Role of Matrix Metalloproteinase 14 in Adipose Tissue Remodeling during Obesity. *Mol. Cell. Biol.* **40**, (2020).

130. Bade, A. N., McMillan, J. E. M., Liu, Y., Edagwa, B. J. & Gendelman, H. E. Dolutegravir Inhibition of Matrix Metalloproteinases Affects Mouse Neurodevelopment. *Mol. Neurobiol.* **58**, 5703–5721 (2021).

131. Jung, I. *et al.* Dolutegravir Suppresses Thermogenesis via Disrupting Uncoupling

Protein 1 Expression and Mitochondrial Function in Brown/Beige Adipocytes in Preclinical Models. *J. Infect. Dis.* 1–11 (2022) doi:10.1093/infdis/jiac175.

132. Rizzardo, S. *et al.* Dolutegravir monotherapy and body weight gain in antiretroviral naïve patients. *Aids* **33**, 1673–1674 (2019).

133. Hernandez-Quiles, M., Broekema, M. F. & Kalkhoven, E. PPARgamma in Metabolism, Immunity, and Cancer: Unified and Diverse Mechanisms of Action. *Front. Endocrinol. (Lausanne).* **12**, 1–17 (2021).

134. Homeostasis, A. *et al.* crossm Peroxisome Proliferator-Activated Receptor ⚡ and Its Role in. 1–15 (2018).

135. Karsdal, M. A. *et al.* The good and the bad collagens of fibrosis – Their role in signaling and organ function. *Adv. Drug Deliv. Rev.* **121**, 43–56 (2017).

136. Reagan-Shaw, S., Nihal, M. & Ahmad, N. Dose translation from animal to human studies revisited. *FASEB J.* **22**, 659–661 (2008).

137. Nair, A. & Jacob, S. A simple practice guide for dose conversion between animals and human. *J. Basic Clin. Pharm.* **7**, 27 (2016).

138. Rhodes, M. *et al.* Assessing a theoretical risk of dolutegravir-induced developmental immunotoxicity in juvenile rats. *Toxicol. Sci.* **130**, 70–81 (2012).

139. Sengupta, P. The laboratory rat: Relating its age with human's. *Int. J. Prev. Med.* **4**, 624–630 (2013).

140. Ghasemi, Asghar; Sajad, J. K. K. Review article : THE LABORATORY RAT : AGE AND BODY WEIGHT MATTER. *EXCLI J. 2021;201431-1445* **2005**, 1431–1445 (2021).

141. Sengupta, P. A scientific review of age determination for labortory rat: how old is it in comparison with human age? *Biomed. Int.* **2**, 81–89 (2011).

142. Charles River. Wistar IGS Rat. https://www.criver.com/products-services/find-model/wistar-igs-rat?region=3651 (2021).

143. Bradford, M. A Rapid and Sensitive Method for the Quantitation of Microgram Quantities of Protein Utilizing the Principle of Protein-Dye Binding. *Anal. Biochem.* **72**, 248–254 (1976).

144. Wang, Z. *et al.* [Estimation of the normal range of blood glucose in rats]. *Wei Sheng Yan Jiu* **39**, 20459020 (2010).

145. Esber, A. L. *et al.* Weight gain during the dolutegravir transition in the African Cohort Study. *J. Int. AIDS Soc.* **25**, e25899 (2022).

146. Dolutegravir-Based or Low-Dose Efavirenz–Based Regimen for the Treatment of HIV-1. *N. Engl. J. Med.* **381**, 816–826 (2019).

147. Couturier, J. *et al.* Adipocytes impair efficacy of antiretroviral therapy. *Antiviral Res.* **154**, 140–148 (2018).

148. Agarwal, N. & Balasubramanyam, A. Viral mechanisms of adipose dysfunction: lessons from HIV-1 Vpr. *Adipocyte* **4**, 55–59 (2015).

149. Koethe, J. R. & Heimburger, D. C. Nutritional aspects of HIV-associated wasting in sub-Saharan Africa. *Am. J. Clin. Nutr.* **91**, 1138–1142 (2010).

150. Kosmiski, L. Energy expenditure in HIV infection. *Am. J. Clin. Nutr.* **94**, 1677–1682 (2011).

151. Takarinda, K. C. *et al.* Malnutrition status and associated factors among HIV-positive patients enrolled in ART clinics in Zimbabwe. *BMC Nutr.* **3**, 1–11 (2017).

152. Quirós Cognuck, S. *et al.* Sex differences in body composition, metabolism-related hormones, and energy homeostasis during aging in Wistar rats. *Physiol. Rep.* **8**, 1–14 (2020).

153. Fuente-Martín, E., Argente-Arizón, P., Ros, P., Argente, J. & Chowen, J. A. Sex differences in adipose tissue. *Adipocyte* **2**, 128–134 (2013).

154. Garcia-Carrizo, F., Priego, T., Szostaczuk, N., Palou, A. & Picó, C. Sexual dimorphism in the age-induced insulin resistance, liver steatosis, and adipose tissue function in rats. *Front. Physiol.* **8**, 1–14 (2017).

155. Fu, Y., Luo, N., Klein, R. L. & Timothy Garvey, W. Adiponectin promotes adipocyte differentiation, insulin sensitivity, and lipid accumulation. *J. Lipid Res.* **46**, 1369–1379 (2005).

156. Gariballa, S., Alkaabi, J., Yasin, J. & Al Essa, A. Total adiponectin in overweight and

obese subjects and its response to visceral fat loss. *BMC Endocr. Disord.* **19**, 1–6 (2019).

157. Achari, A. E. & Jain, S. K. Adiponectin, a therapeutic target for obesity, diabetes, and endothelial dysfunction. *Int. J. Mol. Sci.* **18**, (2017).

158. Johannsen, D. L. *et al.* Effect of 8 weeks of overfeeding on ectopic fat deposition and insulin sensitivity: Testing the 'adipose tissue expandability' hypothesis. *Diabetes Care* **37**, 2789–2797 (2014).

159. Matsuda, M. & Shimomura, I. Roles of adiponectin and oxidative stress in obesity-associated metabolic and cardiovascular diseases. *Rev. Endocr. Metab. Disord.* **15**, 1–10 (2014).

160. Delaney, K. Z. & Santosa, S. Sex differences in regional adipose tissue depots pose different threats for the development of Type 2 diabetes in males and females. *Obes. Rev.* **23**, (2022).

161. Velasco, M. *et al.* Sexual dimorphism in insulin resistance in a metabolic syndrome rat model. *Endocr. Connect.* **9**, 890–902 (2020).

162. Wang, Q. A., Tao, C., Gupta, R. K. & Scherer, P. E. Tracking adipogenesis during white adipose tissue development, expansion and regeneration. *Nat. Med.* **19**, 1338–1344 (2013).

163. Newell-Fugate, A. E. The role of sex steroids in white adipose tissue adipocyte function. *Reproduction* **153**, R133–R149 (2017).

164. Muir, L. A. *et al.* Adipose tissue fibrosis, hypertrophy, and hyperplasia: Correlations with diabetes in human obesity. *Obesity* **24**, 597–605 (2016).

165. Berezin, A. E., Berezin, A. A. & Lichtenauer, M. Emerging Role of Adipocyte Dysfunction in Inducing Heart Failure Among Obese Patients With Prediabetes and Known Diabetes Mellitus. *Front. Cardiovasc. Med.* **7**, 1–20 (2020).

166. Meyer, L. K., Ciaraldi, T. P., Henry, R. R., Wittgrove, A. C. & Phillips, S. A. Adipose tissue depot and cell size dependency of adiponectin synthesis and secretion in human obesity. *Adipocyte* **2**, 217–226 (2013).

167. Haczeyni, F., Bell-Anderson, K. S. & Farrell, G. C. Causes and mechanisms of adipocyte enlargement and adipose expansion. *Obes. Rev.* **19**, 406–420 (2018).

168. Jiang, N., Li, Y., Shu, T. & Wang, J. Cytokines and inflammation in adipogenesis: an updated review. *Front. Med.* **13**, 314–329 (2019).

169. Tormos, K. V. *et al.* Mitochondrial complex III ROS regulate adipocyte differentiation. *Cell Metab.* **14**, 537–544 (2011).

170. Matulewicz, N., Stefanowicz, M., Nikołajuk, A. & Karczewska-Kupczewska, M. Markers of adipogenesis, but not inflammation, in adipose tissue are independently related to insulin sensitivity. *J. Clin. Endocrinol. Metab.* **102**, 3040–3049 (2017).

171. Rolo, A. P., Teodoro, J. S. & Palmeira, C. M. Role of oxidative stress in the pathogenesis of nonalcoholic steatohepatitis. *Free Radic. Biol. Med.* **52**, 59–69 (2012).

172. Carrière, A., Fernandez, Y., Rigoulet, M., Pénicaud, L. & Casteilla, L. Inhibition of preadipocyte proliferation by mitochondrial reactive oxygen species. *FEBS Lett.* **550**, 163–167 (2003).

173. Casimir, G. J., Lefèvre, N., Corazza, F., Duchateau, J. & Chamekh, M. The acid-base balance and gender in inflammation: A mini-review. *Front. Immunol.* **9**, 1–6 (2018).

174. Nakagawa, M., Karim, M. R., Izawa, T., Kuwamura, M. & Yamate, J. Immunophenotypical characterization of M1/M2 macrophages and lymphocytes in cisplatin-induced rat progressive renal fibrosis. *Cells* **10**, 1–15 (2021).

175. Iyer, S. S. & Cheng, G. Role of interleukin 10 transcriptional regulation in inflammation and autoimmune disease. *Crit. Rev. Immunol.* **32**, 23–63 (2012).

176. Zhang, Z. *et al.* Dermal adipose tissue has high plasticity and undergoes reversible dedifferentiation in mice. *J. Clin. Invest.* **129**, 5327–5342 (2019).

177. Wernstedt Asterholm, I. *et al.* Adipocyte inflammation is essential for healthy adipose tissue expansion and remodeling. *Cell Metab.* **20**, 103–118 (2014).

178. Kanda, Y., Hinata, T., Kang, S. W. & Watanabe, Y. Reactive oxygen species mediate adipocyte differentiation in mesenchymal stem cells. *Life Sci.* **89**, 250–258 (2011).

179. Salem, A. M., Latif, R. & Rafique, N. Comparison of adiponectin levels during the

menstrual cycle between normal weight and overweight/obese young females. *Physiol. Res.* **68**, 939–945 (2019).

180. Šrámková, M. *et al.* Levels of adipokines and some steroids during the menstrual cycle. *Physiol. Res.* **64**, S147–S154 (2015).

181. Wyskida, K. *et al.* The levels of adipokines in relation to hormonal changes during the menstrual cycle in young, normal-weight women. *Endocr. Connect.* **6**, 892–900 (2017).

182. Kim, J. H., Cho, H. T. & Kim, Y. J. The role of estrogen in adipose tissue metabolism: Insights into glucose homeostasis regulation. *Endocr. J.* **61**, 1055–1067 (2014).

Appendices

Appendix 1: Ethics approval

UNIVERSITEIT
STELLENBOSCH
UNIVERSITY

Approved with Stipulations

24/06/2021

PI: Dr KS Petersen-Ross

REC: ACU Reference #: ACU-2021-22035

Title: Obesity; a confounder in Dolutegravir treatment?

Dear Dr KS Petersen-Ross

Your response to modifications, with reference number #ACU-2021-22035 was reviewed by the Research Ethics Committee: Animal Care and Use via committee review procedures and was approved on condition that the following stipulations are clarified:

1. A long list of side effects and adverse clinical effects to the drug that will be given is provided; however, the pain and distress category is given as C. Will the animals not require treatment or intervention if they develop these symptoms?

2. Rats will be housed 4 per cage and be given jelly blocks for the drug administration. How will you ensure that each rat get the same amount of drugs?

Applicants are reminded that they are expected to comply with accepted standards for the use of animals in research and teaching as reflected in the South African National Standards 10386: 2008. The SANS 10386: 2008 document is available on the Division for Research Developments website www.sun.ac.za/research.

As provided for in the Veterinary and Para-Veterinary Professions Act, 1982. It is the principal investigator's responsibility to ensure that all study participants are registered with or have been authorised by the South African Veterinary Council (SAVC) to perform the procedures on animals, or will be performing the procedures under the direct and continuous supervision of a SAVC-registered veterinary professional or SAVC-registered para-veterinary professional, who are acting within the scope of practice for their profession.

Please remember to use your REC: ACU reference number: # ACU-2021-22035 on any documents or correspondence with the REC: ACU concerning your research protocol.

If you have any questions or need further help, please contact the REC: ACU office at 021 808 9003.

Visit the Division for Research Developments website www.sun.ac.za/research for documentation on REC: ACU policy and procedures.

Sincerely,

Mr Winston Beukes

Coordinator: Research Ethics (Animal Care and Use)

Appendix 2: Ethics exemption

UNIVERSITEIT·STELLENBOSCH·UNIVERSITY
jou kennisvennoot • your knowledge partner

Ethics Letter

08-Jul-2015

Ethics Reference #: X15/05/013
Title: Use of donated blood (buffy coat) for isolation and preparation of primary monocyte cultures.

Dear Prof Carine Smith,

Thank you for your application to our Health Research Ethics Committee (HREC). The Health Research Ethics Committee considers this proposal to be exempt from ethical review.

This letter confirms that this research is now registered and you can proceed with study related activities.

If you have any queries or need further help, please contact the REC Office 219389207.

Sincerely,

REC Coordinator
Mertrude Davids
Health Research Ethics Committee 2

Appendix 3: DTG purity

Table A: DTG purity. *Number of DTG extractions performed with amount of DTG (mg) obtained from each consecutive extraction as well as purity obtained from HPLC purity analysis. Purity is calculated as the percentage area under curve (AUC) on the chromatogram.*

Extraction no.	Amount of DTG extracted (mg)	Purity
1	20,45	>99,9
2	21,11	>99,9
3	19,85	>99,9
4	18,81	>99,9
5	19,66	>99,9
6	19,53	>99,9
7	19,62	>99,9
8	63,56	>99,9
9	65,88	>99,9
10	66,58	>99,9
11	65,53	>99,9
12	63,48	>99,9
13	57,67	>99,9
14	79,17	>99,9
15	82,47	>99,9
16	90,51	>99,9
17	74,47	>99,9
18	85,54	>99,9
19	63,50	>99,9
20	10,93	>99,9
21	55,83	>99,9
22	17,28	>99,9
23	36,69	>99,9
24	44,95	>99,9
25	62,82	>99,9
26	54,49	>99,9
27	22,63	>99,9
28	68,20	>99,9
29	60,48	>99,9
30	58,85	>99,9
31	55,01	>99,9
32	34,65	>99,9
33	53,87	>99,9
34	55,19	>99,9
35	49,75	>99,9
36	61,39	>99,9

37	55,81	>99,9
38	62,43	>99,9